Discrimination of aliphatic and aromatic hydrocarbons *via* modulated folding and fluorescence of an NDI-tetramer

Dhanyashree Das,[a] Dhrubajyoti Talukdar [a] and Bappaditya Gole*[a]

[a]*Biomimetic Supramolecular Chemistry Laboratory, Department of Chemistry, School of Natural Sciences, Shiv Nadar Institution of Eminence Deemed to be University, Greater Noida, Uttar Pradesh 201314, India.*

E-mail: bappaditya.gole@snu.edu.in

Supplementary Information

Content **Page Number**

1. Materials and Methods 2 - 3
2. Synthetic Procedures 3 - 8
3. Characterization 9 - 16
4. Solvent-Dependent Studies
   - 4.1. UV-Vis for aliphatic solvents 16 - 17
   - 4.2. UV-Vis for aromatic solvents 18-19
   - 4.3. Fluorescence for aliphatic solvents 20-22
   - 4.4. Fluorescence for aromatic solvents 22-23
   - 4.5. Lifetime measurements 24-25
5. NMR spectra of the synthesized compounds 26-33
6. References 33

1. Materials and methods

1.1. General Information

All the Solvents and chemicals were purchased from Sigma-Aldrich, TCI Chemicals, Alfa-Aesar, Rankem, or BLD Chemicals and were used without further purification. The pyridine derivatives were prepared considering reported procedures for similar derivatives.[1] Tetrahydrofuran (THF) and dichloromethane (CH_2Cl_2) were dried over alumina columns (MBRAUN SPS-800 solvent purification system); ethyl acetate (EtOAc), and diisopropylethylamine (DIPEA) were distilled over calcium hydride (CaH_2), before use. Anhydrous DMF was purchased from Sigma Aldrich and used as it is without any further treatment. Reactions were monitored by thin-layer chromatography (TLC) on Merck silica gel 60-F254 plates and observed under UV light. Column chromatography purifications were performed using silica gel (100-200 mesh) unless mentioned otherwise. Preparative recycling GPC (gel permeation chromatography) was performed on the Japan Analytical Industry (JAI) LaboACE LC-5060 instrument using JAIGEL-2HR and JAIGEL-2.5HR (20×600 mm) columns at a flow rate of 7 mL/min with a mobile phase composed of 1% (vol/vol) ethanol and 0.1% (vol/vol) Et_3N in chloroform. Monitoring was carried out by a UV detector at 254 nm, 300 nm, 400 nm, and 500 nm.

1.2. Nuclear Magnetic Resonance

NMR spectra were recorded on a Bruker Avance III HD 400 NMR spectrometer operating at 400 MHz for ^1H spectra and 100 MHz for ^{13}C spectra. Chemical shifts (δ) are reported in parts per million (ppm) relative to the residual proton signal of the deuterated solvent used. ^1H-NMR splitting patterns with observed first-order coupling are designated as singlet (s), doublet (d), triplet (t), quartet (q) or multiplet (m). Coupling constants (J) are reported in hertz. Samples were not degassed otherwise. Data processing was performed with Topspin software 4.3.0.

1.3. Mass Spectroscopy

High-resolution ESI mass spectra (HR-MS) were recorded using an Agilent 6540 UHD Accurate-Mass Q-TOF LC/MS system, and the following are the operation parameters: temperature 350 °C, dry nitrogen gas flow rate 10 L/min, nebulizer pressure 30 psi, Vcap 4000 and fragmentor voltage 100 V. Mass spectra were acquired in the positive ion mode. Accurate mass analysis calibration was carried out by ESI-low concentration tuning mix solution provided by Agilent technologies, U.S.A. The accuracy error threshold was set at 5 ppm. MALDI-TOF mass spectra were recorded using Bruker Autoflex maX MALDI TOF/TOF instrument. The matrix used was α-Cyano-4-hydroxycinnamic acid (CHCA).

1.4. Spectroscopic Methods

Electronic absorption spectra were measured on a JASCO V-750 UV-Vis spectrophotometer. Variable temperature UV-Vis was carried out using Peltier temperature control. Steady-state fluorescence measurements were carried out using a fluorimeter (Fluoromax Plus, Horiba) equipped with a standard cuvette holder fitted with a PMT (185-800) detector and excited with

a 150W CW Ozone-free xenon arc lamp. All solvents used were spectroscopic grade. Chloroform was treated with K_2CO_3 before usage to avoid protonation of any kind. Time-resolved fluorescence decay measurements of the samples were performed using a time-correlated single photon counting instrument (LifeSpec-II, Edinburgh Instruments, Livingston, U.K.) equipped with a 375 nm excitation source and an MCP PMT detector.

The absolute quantum yields of the samples were measured in FLS1000 with a QYPro integrating sphere. Synchronous scans of the sample and reference are converted into reflectance of absorbance in the Fluoracle software. The absolute quantum yield of **1** and **10** was measured in $CHCl_3$, and then after the addition of 50% cyclohexane and toluene.

1.5. Electrochemical measurements

Electrochemical measurements were conducted on BioLogic SP 300 in a three-electrode cell. Cyclic voltammetry (CV) and Differential Pulse Voltammetry (DPV) of the compounds were recorded with glassy carbon as working electrode (WE), Pt as counter electrode (CE), and $Ag/AgNO_3$ as reference electrode (RE). CV and DPV were recorded using 0.1 M NBu_4PF_6 as a supporting electrolyte and anhydrous DCM as a solvent. The experiments were done under Argon conditions and at room temperature. The data were reported with respect to the Fc/Fc^+ (Fc: Ferrocene).

1.6. Computational Methods and Details

Geometry optimisation of **1** was performed using the Forcite module in Material Studio 2020 (BIOVIA Dassault Systèmes). The optimisation was conducted with an iteration number of 5000, using Universal force field to obtain the lowest energy configuration.[2]

2. Synthetic Procedures

The amide linkages are expected to participate in H-bonding with the endocyclic pyridine nitrogen, which generally facilitates folding of the oligomers. Therefore, the initial design strategy was a fully amide-linked NDI-tetramer. However, it required desymmetrization of the NDI monomer, with a protected amine on one end and a free amine on the other. However, repeated attempts to desymmetrize the NDI unit with orthogonal amine protection failed due to the inseparable by-products. This forced us to consider a mixed ester and amide oligomer, which is straightforward to produce. Our studies also revealed that the ester linkages are sufficiently stable and allows further functionalization.

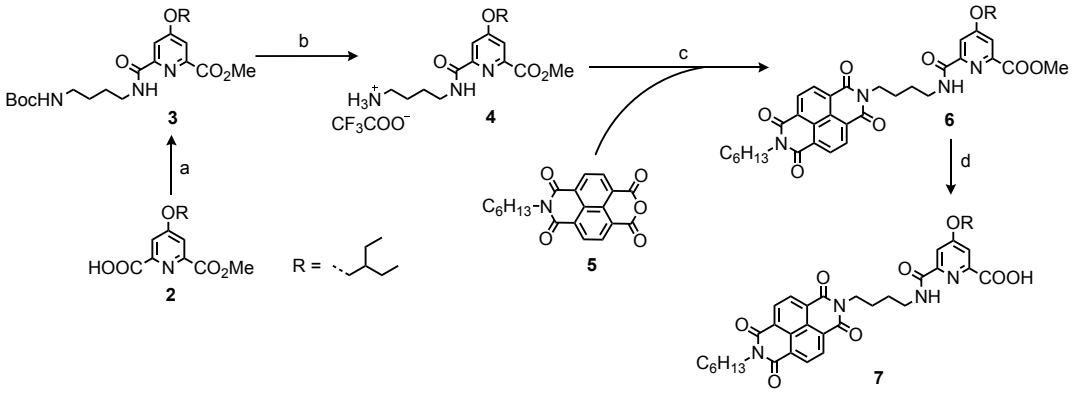

Scheme S1 Synthesis of NDI block **7**. (a) (i) Oxalyl chloride, dry DCM, room temperature, 3 hours; (ii) N-Boc-1,4-butanediamine, dry THF, dry DIPEA, room temperature, 2 hours, 85%, (b) TFA:DCM (1:2), room temperature, 3 hours, 99%, (c) **5**, dry DIPEA, dry DMF, 105 °C, 15 hours, 58%, (d) LiI, dry ethyl acetate, reflux, 15 hours, 83%.

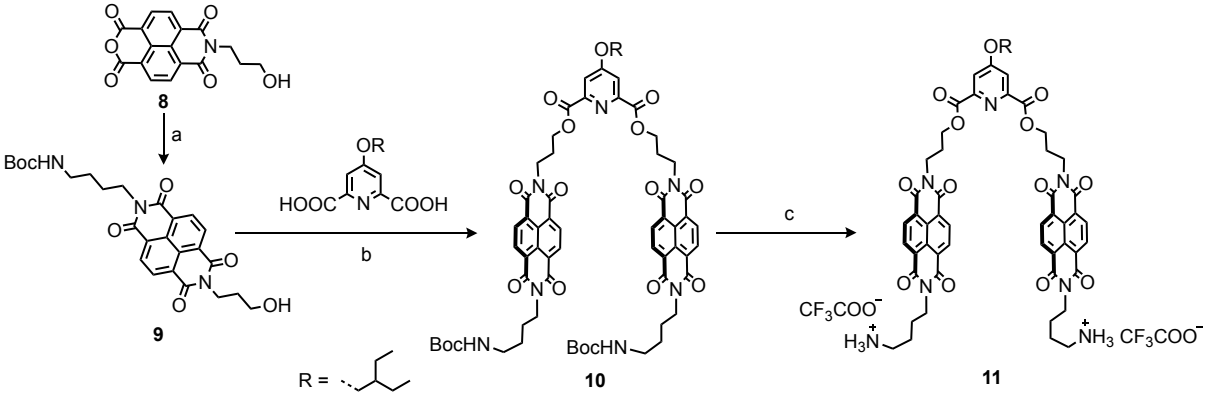

Scheme S2 Synthesis of NDI-dimer block, **11**. (a) N-Boc-1,4-butanediamine, dry DMF, 100 °C, 14 hours, 52%, (b) Py-diacid, HBTU, dry DIPEA, dry DCM, 14 hours, 41%. (c) TFA: DCM (1:1), room temperature, 3 hours, 98%.

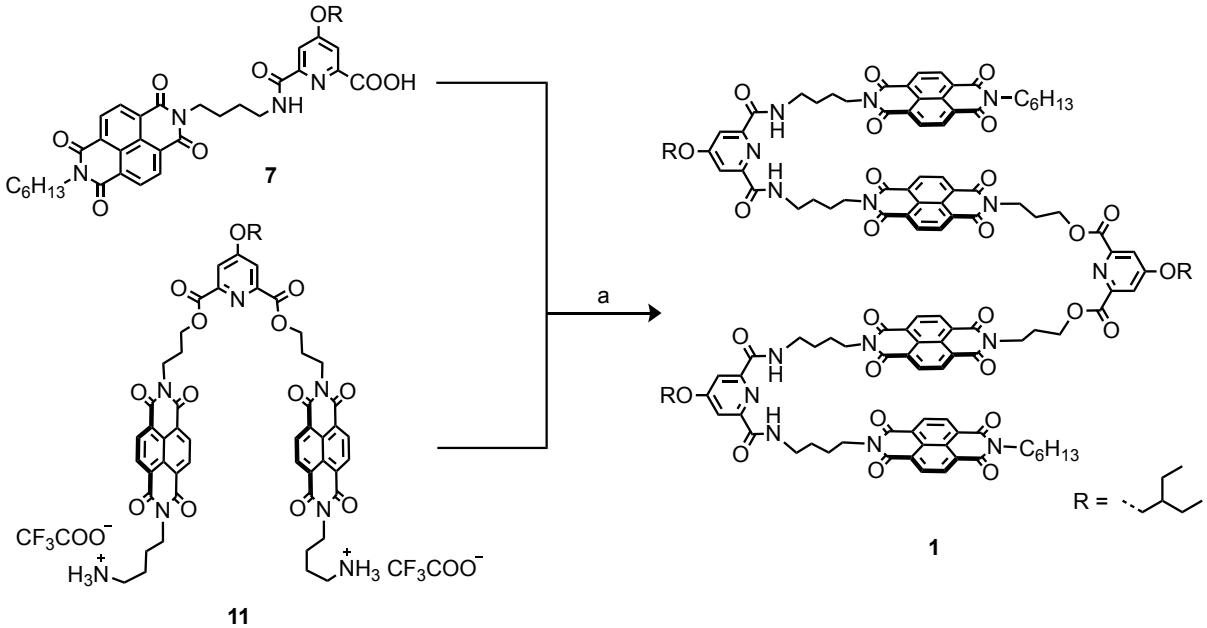

Scheme S3 Synthesis of oligomer **1**. (a) EDC, HOBt, dry DIPEA, dry DCM, room temperature, 12 hours, 20%.

***Methyl6-((4-((tert-butoxycarbonyl)amino)butyl)carbamoyl)-4-(2-ethylbutoxy) picolinate,* 3:**

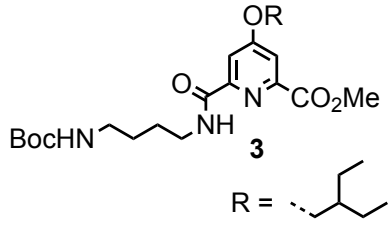

In a 25 mL round-bottom flask, **2** (0.5 g, 1.76 mmol, 1 eq) was taken and dissolved in 2 mL of anhydrous DCM. Oxalyl chloride (2.24 g, 17.6 mmol, 1.5 mL, 10 eq.) was added dropwise in iced-cold conditions and stirred at room temperature for 3 hours under N_2 conditions. Excess oxalyl chloride, along with DCM, was then removed under high vacuum for a duration of 3 hours. The acid chloride formed was used as it is, without further purification, for the next coupling reaction. In another 10 mL round-bottom flask, N-boc-1,4 butanediamine (0.33 g, 1.76 mmol, 1 eq) was dissolved in 5 mL of anhydrous THF, and anhydrous DIPEA (1.8 g, 14.08 mmol, 2.4 mL, 8 eq) was added and transferred dropwise to the acid chloride, which was pre-dissolved in 5 mL of anhydrous THF at 0 °C. The reaction was carried out at room temperature for 2 hours. TLC (DCM: MeOH; 95:5) was checked in between to follow the progress of the reaction. After completion of the reaction, the solvent was evaporated under vacuum and redissolved in DCM. The organic part was washed with 5% citric acid and water. The combined organic layer was dried with Na_2SO_4 and concentrated under reduced pressure. The crude obtained was purified by column chromatography using DCM: MeOH (95:5) as eluent. The pure product was obtained as a viscous yellow liquid. Yield: (85%, 0.677 g). ^{1}H NMR (400 MHz, $CDCl_3$, 298 K) δ 8.15 (t, J = 5.7 Hz, 1H), 7.86 (d, J = 1.5 Hz, 1H), 7.70 (d, J = 1.5 Hz, 1H), 4.59 (s, 1H), 4.02 (m, 5H), 3.50 (q, J = 6.7 Hz, 2H), 3.16 (q, J = 6.1 Hz, 2H), 1.72 (m, 3H), 1.60 (m, 2H), 1.58 (m, 13H), 0.94 (t, J = 7.4 Hz, 6H). ^{13}C{1H} NMR (100 MHz, $CDCl_3$, 298 K) δ 167.6, 165.1, 163.6, 155.9, 152.1, 147.9, 114.7, 110.7, 71.1, 52.9, 40.6, 40.3, 39.2, 28.4, 27.6, 27.1, 23.2, 11.1. HRMS (ESI): m/z calcd for $C_{23}H_{38}N_3O_6$ $[M+H]^+$ 452.2755, Found 452.2757.

***4-(4-(2-ethylbutoxy)-6-(methoxycarbonyl)picolinamido)butan-1-aminium trifluoroacetate,* 4:** In a 25 mL round bottom flask, **3** (0.672 g, 1.49 mmol, 1 eq) was taken and dissolved in 6 mL of DCM. TFA (3 mL) was then added dropwise and stirred at room temperature for 3 hours under N_2 conditions. TLC was checked to monitor the progress of the reaction. After completion, excess TFA, along with DCM, was removed by vacuum and further dried for 3 hours at room temperature. It was then used without purification for the next reaction. The product is obtained as a viscous yellow liquid. Yield: (0.66 g, 99%). ^{1}H NMR (400 MHz, $CDCl_3$, 298 K) δ 8.64 (t, J = 5.9 Hz, 1H), 7.82 (d, J = 1.7 Hz, 1H), 7.74 (d, J = 1.9 Hz, 1H), 7.67 (s, 3H), 4.06 (m, 5H), 3.55 (m, 2H), 3.17 (m, 2H), 1.80 (m, 5H), 1.53 (m, 4H), 0.96 (t, J = 7.4 Hz, 6H). ^{13}C{1H} NMR (100 MHz, $CDCl_3$, 298 K) 168.5, 165.1, 164.8, 161.2, 160.8, 160.4, 159.9, 150.6, 147.3, 116.7, 115.1, 113.8, 111.4, 71.6, 53.3, 40.6, 39.9, 38.8, 23.2, 10.9. $C_{18}H_{30}N_3O_4$ $[M+H]^+$ 352.2231, Found 352.2286.

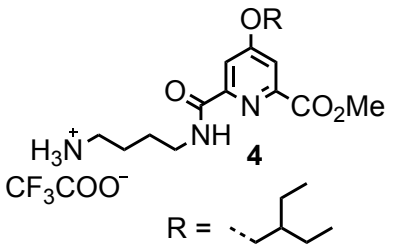

***Methyl4-(2-ethylbutoxy)-6-((4-(7-hexyl-1,3,6,8-tetraoxo-3,6,7,8tetrahydrobenzo[lmn] [3,8]phenanthroline-2(1H)-yl) butyl) carbamoyl) picolinate,* 6:** In a 25 mL round bottom flask, **4** (0.680 g, 1.46 mmol, 1 eq.) and NDI-monohexylanhydride, **5** (0.614 g, 1.75 mmol, 1.2 eq)[3] was taken. Anhydrous DMF (8 mL) was transferred into the 25 mL round-bottom flask under N_2, and the dispersion was stirred for 10 minutes. Subsequently, DIPEA (0.188 g, 1.46 mmol, 0.2 mL, 1 eq) was then added to the mixture, and it was further stirred at 105 °C for 15 hours. TLC was performed in DCM:EtOAc (80:20) to follow the progress of the reaction. Once finished, DMF was removed under vacuum, and ice-cold water was added to the crude reaction mixture. The precipitate formed was then filtered off by vacuum filtration and further washed with minimum amount of methanol. The precipitate was subjected to column chromatography (230-400 mesh) with DCM as an eluent to obtain the pure product as an off-white solid. Yield: (0.573 g, 58%). ^{1}H NMR (400 MHz, $CDCl_3$, 298 K) δ 8.74 (s, 4H), 8.19 (t, J = 6.2 Hz, 1H), 7.84 (d, J = 2.3 Hz, 1H), 7.69 (d, J = 2.3 Hz, 1H), 4.27 (t, J = 7.1 Hz, 2H), 4.20 (m, 2H), 4.01 (m, 5H), 3.58 (q, J = 6.6 Hz, 2H), 1.89 (m, 2H), 1.80 (m, 5H), 1.66 (m, 10H), 0.96 (m, 9H). ^{13}C{1H} NMR (100 MHz, $CDCl_3$, 298 K) δ 167.6, 165.1, 163.7, 162.8, 162.7, 152.1, 148.0, 130.9, 130.8, 126.7, 126.6, 126.6, 114.7, 110.7, 71.1, 52.8, 40.9, 40.6, 40.4, 39.2, 31.5, 28.0, 27.3, 26.7, 25.6, 23.2, 22.5, 13.9. HRMS (ESI): m/z calcd for $C_{38}H_{45}N_4O_8$ $[M+H]^+$ 685.3232, Found 685.3257.

***4-(2-ethylbutoxy)-6-((4-(7-hexyl-1,3,6,8-tetraoxo-3,6,7,8-tetrahydrobenzo [lmn] [3,8] phenanthrolin-2(1H)-yl)butyl)carbamoyl)picolinic acid,* 7:** In a 25 mL round bottom flask, **6,** (0.525 g, 0.767 mmol, 1 eq) was taken along with LiI (0.408 g, 3.070 mmol, 4 eq) and kept under vacuum for an hour. Anhydrous EtOAc (7 mL) was transferred under N_2, and the reaction mixture was refluxed for 15 hours at 77 °C. TLC (DCM:EtOAC; 80:20) was performed to follow the reaction. After the completion, EtOAc was evaporated to dryness under vacuum, and diethyl ether was added. The precipitate formed was then filtered through vacuum filtration and dried over a desiccator. The precipitate was then stirred in 5% citric solution, filtered off, and dried in a vacuum oven at 70 °C to obtain the product as an off white solid. Yield: (0.436 mg, 83%). ^{1}H NMR (400 MHz, $CDCl_3$, 298 K) δ 8.89 (d, J = 7.6 Hz, 2H), 8.81 (d, J = 7.6 Hz, 2H), 8.73 (t, J = 5.6 Hz, 1H), 7.99 (d, J = 2.2 Hz, 1H), 7.87 (d, J = 2.3 Hz, 1H), 4.31 (m, 2H), 4.21 (m, 2H), 4.07 (d, J = 5.7 Hz, 2H), 3.77 (m, 2H), 1.96 (m, 2H), 1.83 (m, 2H), 1.74 (m, 4H), 1.55 (m, 4H), 1.35 (m, 5H), 0.95 (m, 9H). ^{13}C{1H} NMR (100 MHz, $CDCl_3$, 298 K) 168.6, 164.0, 163.7, 163.0, 162. 6, 151.3, 147.1, 131.7, 131.1, 127.1, 126.7, 126.6, 126.1, 112.9,112.7, 71.6, 41.1, 40.6, 39.8, 38.7, 31.5, 28.0, 26.7, 25.0, 24.7, 23.2, 22.5, 14.0, 11.0. HRMS (ESI): m/z calcd for $C_{37}H_{43}N_4O_8$ $[M+H]^+$ 671.3075, Found 671.3084.

tert-butyl(4-(7-(3-hydroxypropyl)-1,3,6,8-tetraoxo-3,6,7,8-tetrahydrobenzo[lmn][3,8]

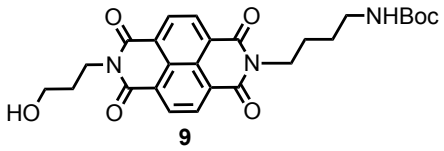

9

***phenanthrolin-2(1H)-yl)butyl)carbamate,* 9:** In a 25 mL round bottom flask, **8** (1 g, 3.07 mmol, 1 eq)[4] was taken along with N-boc 1,4-butanediamine (0.577 g, 3.07 mmol, 1 eq) and 10 mL of DMF was added which lead to a formation of a suspension. It was then heated to 100 °C for 14 hours. Ice-cold water was poured into the crude product, and the precipitate formed was filtered by vacuum filtration. It was washed with brine, water, and methanol to obtain a light pink solid. Yield: (0.773 g, 52%). ^{1}H NMR (400 MHz, $CDCl_3$, 298 K) δ 8.79 (m, 4H), 4.61 (s, 1H), 4.39 (t, J = 6.3 Hz, 2H), 4.23 (t, J = 7.4 Hz, 2H), 3.65 (t, J = 5.6 Hz, 2H), 3.22 (m, 2H), 2.04 (m, 2H), 1.82 (m, 2H), 1.65 (m, 2H), 1.42 (s, 9H). ^{13}C{1H} NMR (100 MHz, $CDCl_3$, 298 K) 163.6, 162.9, 131.4, 131.2, 126.9, 126.8, 126.4, 59.3, 40.6, 37.6, 31.1, 28.5, 27.8, 25.5. HRMS (ESI): m/z calcd for $C_{26}H_{29}N_3O_7Na$ $[M+Na]^+$ 518.1898, Found 518.1894.

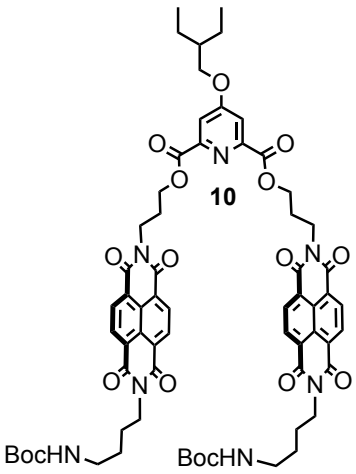

10

***bis(3-(7-(4-((tert-butoxycarbonyl)amino)butyl)-1,3,6,8-tetraoxo-3,6,7,8-tetrahydrobenzo [lmn][3,8]phenanthrolin-2(1H)-yl)propyl) 4-(2-ethylbutoxy) pyridine-2,6-dicarboxylate,* 10:** In a 25 mL round-bottom flask, pyridine-diacid (0.150 g, 0.56 mmol, 1 eq),[1] **9** (0.555 g, 1.12 mmol, 2 eq), and HBTU (0.637 g, 1.68 mmol, 3 eq) were taken and kept in a vacuum for 30 minutes. Anhydrous DCM (3 mL) and anhydrous DIPEA (0.217 mg, 1.68 mmol, 0.3 mL, 3 eq) were added to the mixture under N_2 conditions and stirred at room temperature for 14 hours. The progress of the reaction was monitored by TLC using DCM:MeOH (95:5). The reaction was quenched by removing DCM under reduced pressure, and MeOH was added to precipitate out the compound. The compound was further purified by gel permeation chromatography to get the pure product as an off-white solid. Yield: (0.290 g, 41%). ^{1}H NMR (400 MHz, $CDCl_3$, 298 K) δ 8.61 (m, 8H), 7.64 (s, 2H), 4.70 (s, 2H), 4.46 (m, 8H), 4.19 (t, J = 7.3 Hz, 4H), 4.01 (d, J = 5.7 Hz, 2H), 3.22 (m, 4H), 2.30 (m, 4H), 1.83 (m, 4H), 1.67 (m, 5H), 1.59 (m, 4H), 1.42 (s, 18H), 0.98 (t, J = 7.4 Hz, 6H). ^{13}C{1H} NMR (100 MHz, $CDCl_3$, 298 K) 167.7, 163.9, 162.8, 162.6, 156.4, 150.8, 136.6, 130.9, 130.9, 128.5, 128.0, 126.5, 126.5, 126.4, 111.7, 78.9, 66.6, 46.1, 40.6, 40.5, 40.4, 39.3, 33.2, 27.5, 27.2, 26.7, 25.5, 25.3, 22.6, 13.9, 10.9. HRMS (ESI): m/z calcd for $C_{65}H_{72}N_7O_{17}$ $[M+H]^+$ 1223.4906, Found 1223.4978.

4,4'-((((4-(2-ethylbutoxy)pyridine-2,6-dicarbonyl)bis(oxy))bis(propane-3,1-diyl))bis(1,3,6,8-tetraoxo-3,6,7,8-tetrahydrobenzo[*lmn*][3,8]phenanthroline-7,2(1*H*)-diyl))bis(butan-1-aminium) trifluoroacetate 11, In a 10 mL round-bottom flask, **10** (0.2 g, 0.16 mmol, 1 eq) was taken and dissolved in 2 mL of DCM. TFA (2 mL) was added to the reaction mixture dropwise and the reaction was then stirred at room temperature for 3 hours under N_2 conditions. The TLC (DCM: MeOH; 95:5) was checked in between to confirm the completion of the reaction. The reaction mixture was then evaporated under reduced pressure and dried under vacuum for 3 hours. The compound was then used for the further reaction without purification. Yield (0.196 g, 98%). ^{1}H NMR (400 MHz, DMSO-d_6, 298 K) δ 8.49 (q, J=7.6 Hz, 8H), 7.67 (s, 6H), 7.43 (s, 2H), 4.34 (m, 4H), 4.27(t, J = 6.4 Hz, 6H), 4.08 (t, J = 7.0 Hz, 4H), 3.99 (d, J = 5.7 Hz, 2H), 3.12 (m, 2H), 2.89 (m, 2H), 2.15 (m, 4H), 1.75 (m, 4H), 1.67 (m, 5H), 1.49 (m, 4H), 0.94 (t, J = 7.5 Hz, 6H). ^{13}C{1H} NMR (100 MHz, $CDCl_3$, 298 K) 166.5, 164.3, 162.9, 162.8, 158.9, 158.6, 149.5, 130.7, 130.6, 126.5, 126.2, 126.0, 117.5, 114.6, 114.0, 64.8, 52.5, 46.2, 26.6, 25.2, 25.1, 23.1, 11.3, 9.1, 7.6.

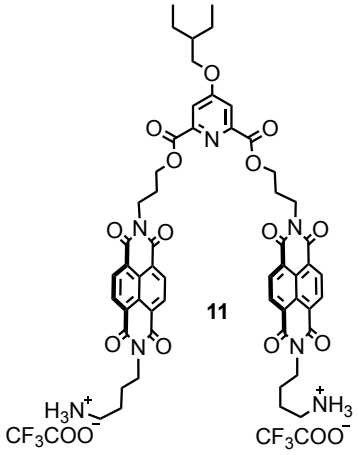

***NDI tetramer,* 1:** In a 10 mL round-bottom flask, **7** (0.157 g, 0.23 mmol, 2 eq.) was taken along with EDC.HCl (0.178 g, 0.93 mmol, 4 eq) and HoBT (0.148 g, 0.92 mmol, 4 eq) and kept in a vacuum for 30 minutes. Under N_2, anhydrous DCM (2 mL) and anhydrous DIPEA (0.241 g, 1.84 mmol, 0.34 mL, 8 eq) were added to it. In another 10 mL, the salt of **11** (0.146 g, 0.117 mmol, 1 eq**)** was also dispersed in anhydrous DCM (1 mL) and then transferred to the former RB under N_2 conditions. The reaction mixture was stirred at room temperature for 12 hours. DCM was then completely evaporated under reduced pressure. To the crude mixture, methanol was added to precipitate out the compound. It was then purified by column chromatography using DCM:acetonitrile (90:10) and later by Gel Permeation Chromatography (GPC) to get an off-white solid. Yield: (0.054 g, 20%). ^{1}H NMR (400 MHz, $CDCl_3$, 298 K) δ 8.70 (m, 8H), 8.52 (m, 8H), 8.36 (m, 4H), 7.76 (s, 4H), 7.65 (s, 2H), 4.45 (m, 8H), 4.17 (m, 8H), 4.10 (m, 4H), 4.00 (d, J = 5.6 Hz, 2H), 3.93 (d, J = 5.6 Hz, 4H), 3.56 (m, 8H), 2.27 (m, 4H), 1.78 (m, 20H), 1.54 (m, 4H), 1.46 (m, 14H), 1.33 (m, 6H), 0.96 (t, J = 7.4 Hz, 6H) 0.88 (t, J = 7.4 Hz, 18H). ^{13}C{1H} NMR (100 MHz, $CDCl_3$, 298 K) 167.7, 163.9, 162.8, 162.6, 150.8, 130.9, 126.7, 126.5, 126.4, 126.3, 111.7, 79.0, 45.8, 41.0, 40.5, 39.3, 33.2, 31.5, 29.7, 28.0, 27.2, 27.2, 26.8, 26.7, 25.6, 22.6, 22.5, 14.0, 13.9. MALDI-TOF: m/z calcd for $C_{129}H_{135}N_{15}NaO_{27}$ $[M+Na]^+$ 2349.9578 Found 2349.9611.

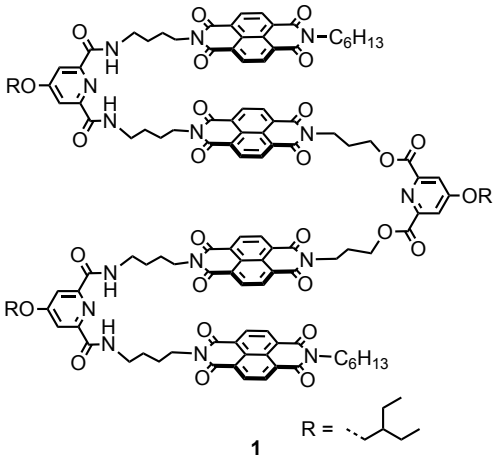

3. Characterization

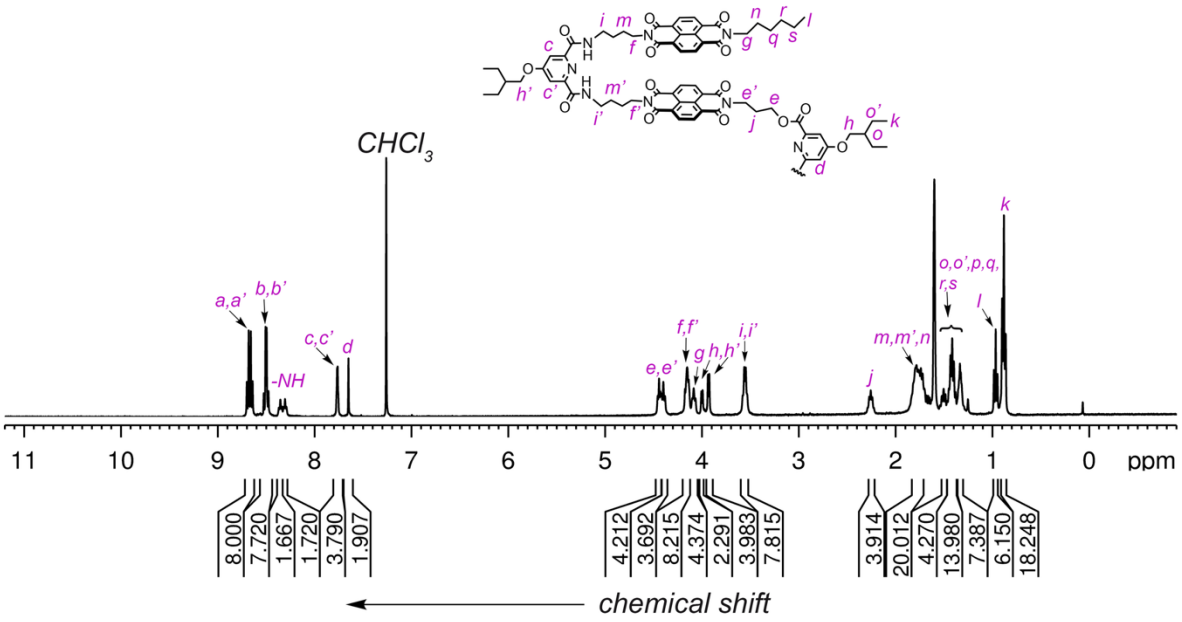

Fig. S1 400 MHz ^{1}H-NMR of **1** in $CDCl_3$ at 298 K with peak assignment.

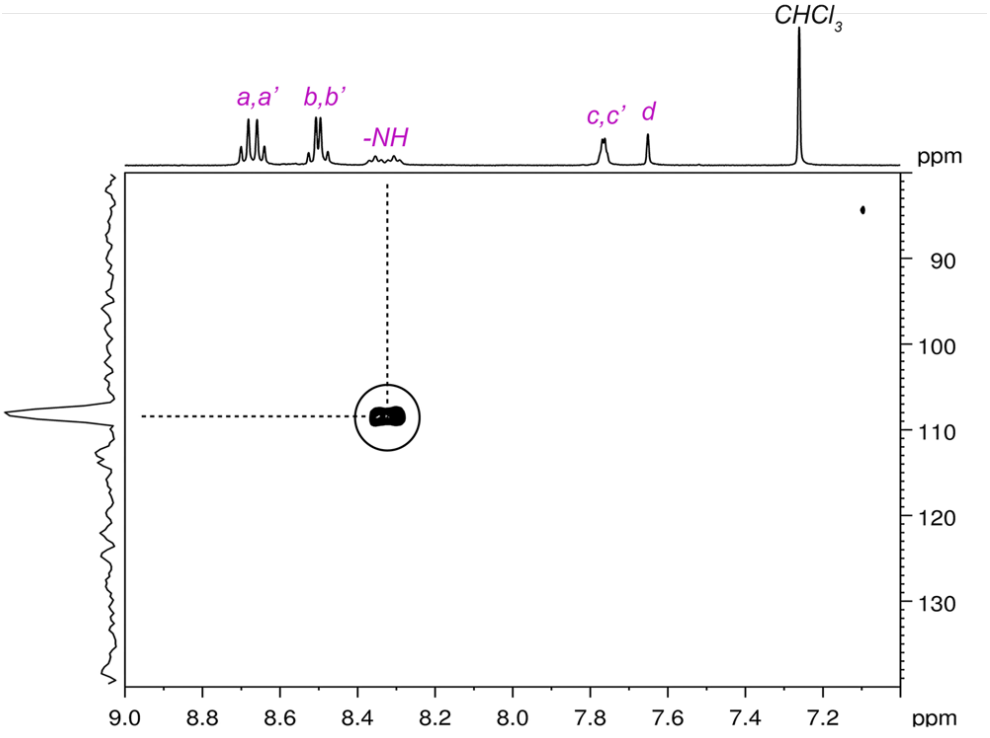

Fig. S2 400 MHz ^{1}H-^{15}N HSQC NMR spectra of **1** in $CDCl_3$ at 298 K.

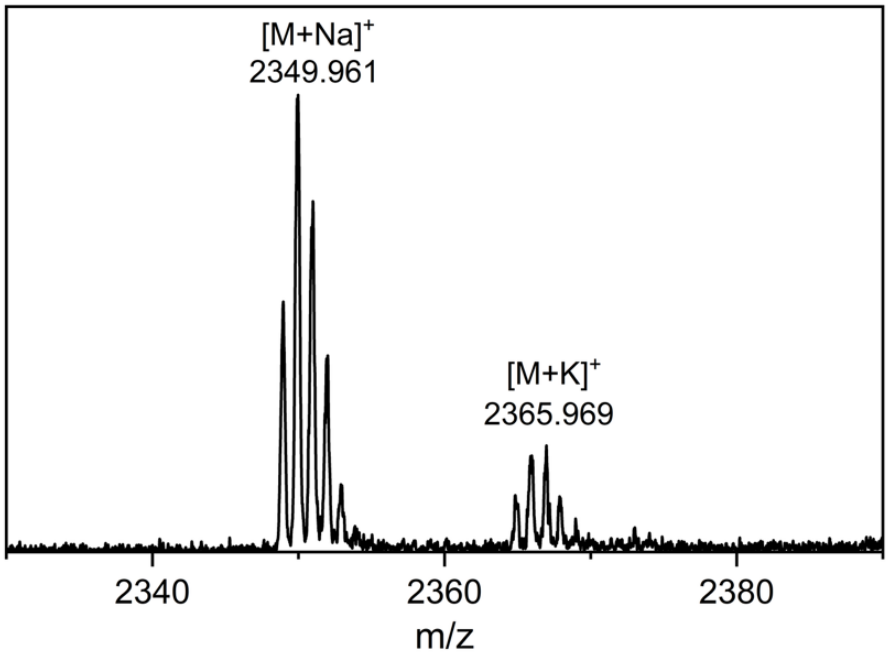

Fig. S3 MALDI-TOF mass spectra of **1**.

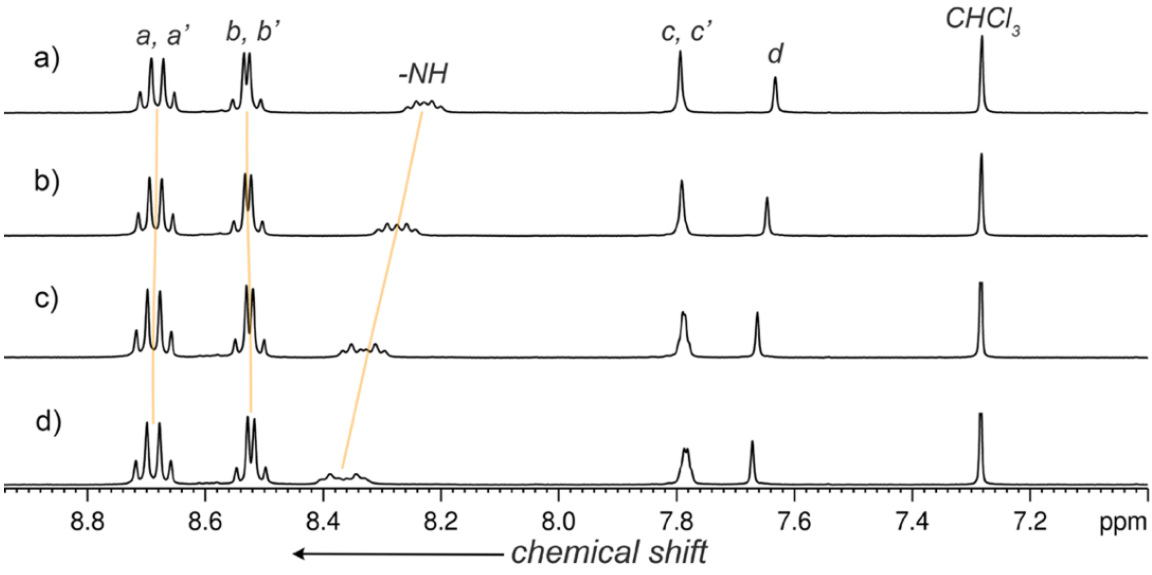

Fig. S4 Partial 400 MHz temperature-dependent ^{1}H NMR of **1** (5 mM) in $CDCl_3$ at (a) 323 K, (b) 313 K, (c) 303 K, (d) 298 K.

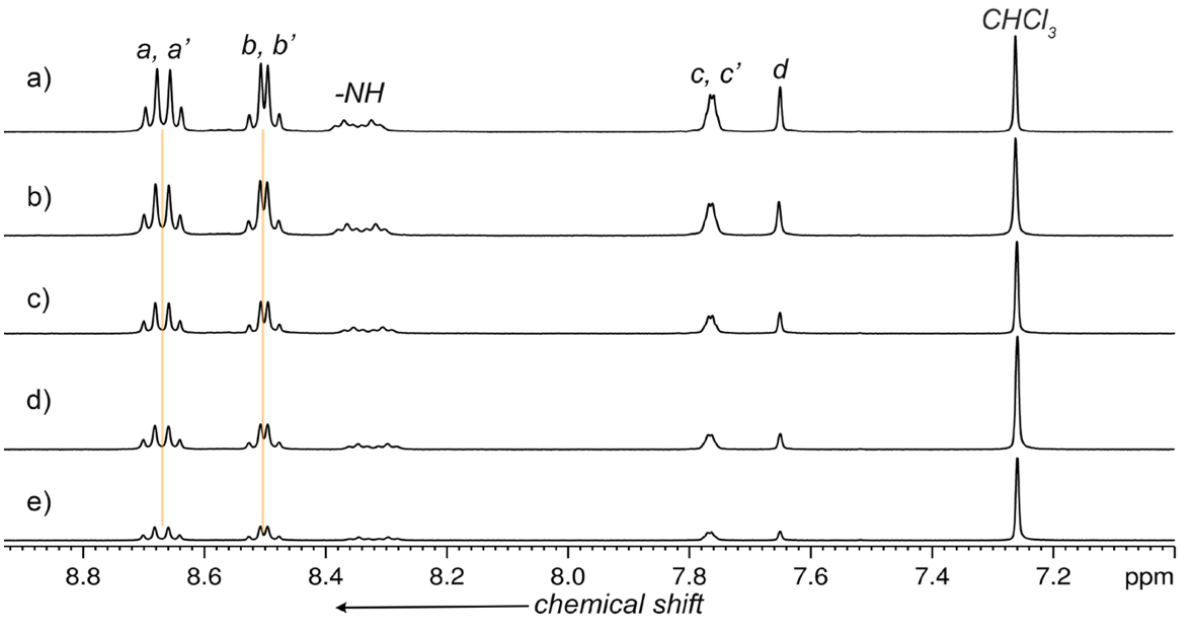

Fig. S5 Partial 400 MHz concentration-dependent ^{1}H NMR of **1** (a) 5 mM, (b) 3 mM, (c) 2 mM, (d) 1 mM, (e) 0.5 mM in $CDCl_3$ at 298 K.

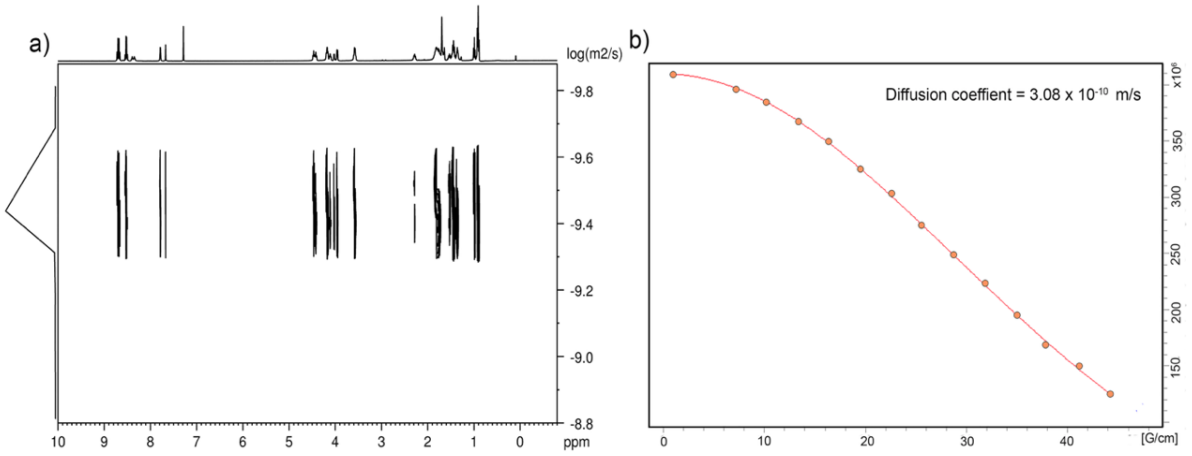

Fig. S6 (a) ^{1}H DOSY spectrum of **1** (2 mM) in $CDCl_3$ at 298 K, (b) The diffusion coefficient was calculated from the processed experimental DOSY spectrum with the TopSpin 3.6.3 T1/T2 software. The circles represent ^{1}H-NMR peak intensities as a function of increasing gradient strength, and the red line represents the regression fit. The solvodynamic diameter, d_s = 27 Å was calculated using the Stokes-Einstein equation.

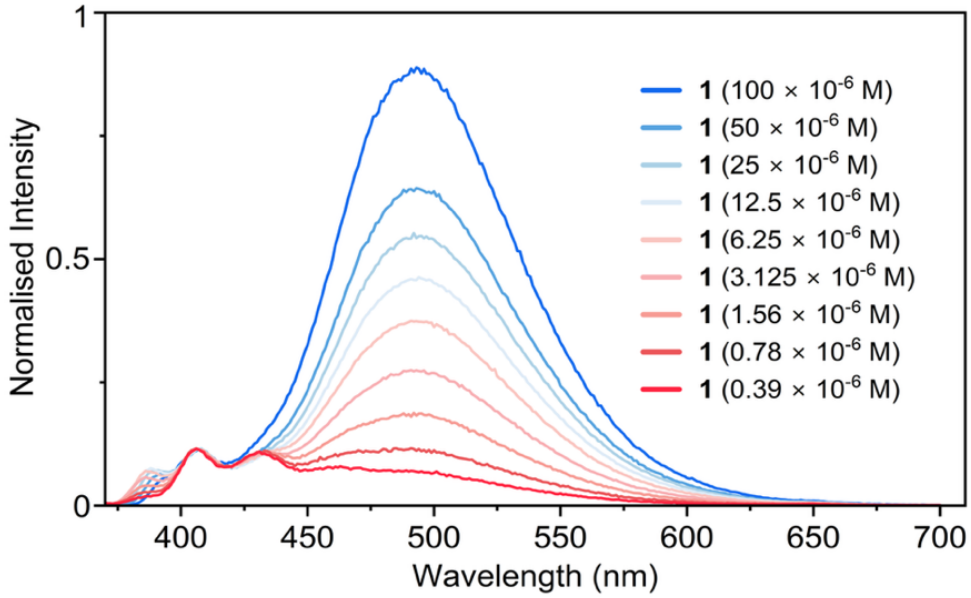

Fig. S7 Normalized concentration-dependent steady-state emission spectra (normalized at 407 nm) of **1** in $CHCl_3$ at 298 K (λ_{ex} = 360 nm). The excimer-like emission persists in sub-micromolar concentration which indicates it is an intramolecular phenomenon.

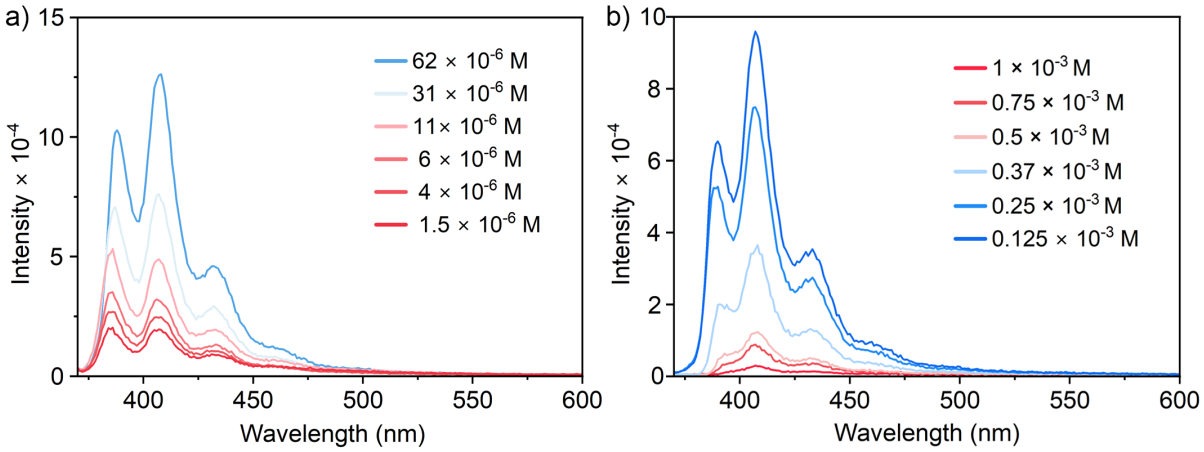

Fig. S8 Concentration-dependent fluorescence of the reference compound NDI-ref. (a) The low concentration regime (1.5 – 62 × 10^{-6} M) shows an increase in the monomeric emission band. (b) The high concentration regime (62 × 10^{-6} M to 1 × 10^{-3} M) shows quenching of the monomeric emission, probably due to the aggregation-induced quenching. However, the excimer emission could not be seen within this wide concentration range.

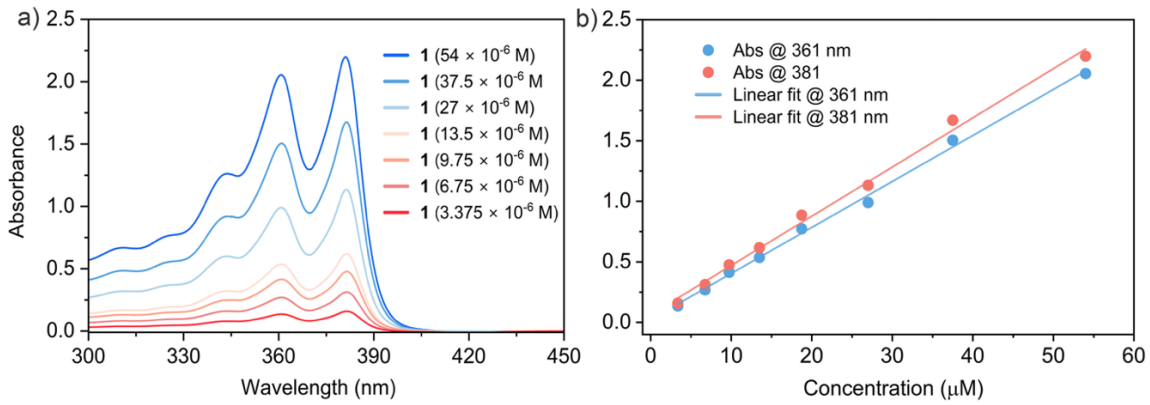

Fig. S9 (a) Concentration-dependent UV-vis spectra of **1** in $CHCl_3$ at 298 K; path length: 5 mm. There are no significant spectral changes with the increase in concentration. (b) The concentration vs absorbance plot shows a linear relationship, which confirms the non-existence of molecular association in this concentration range.

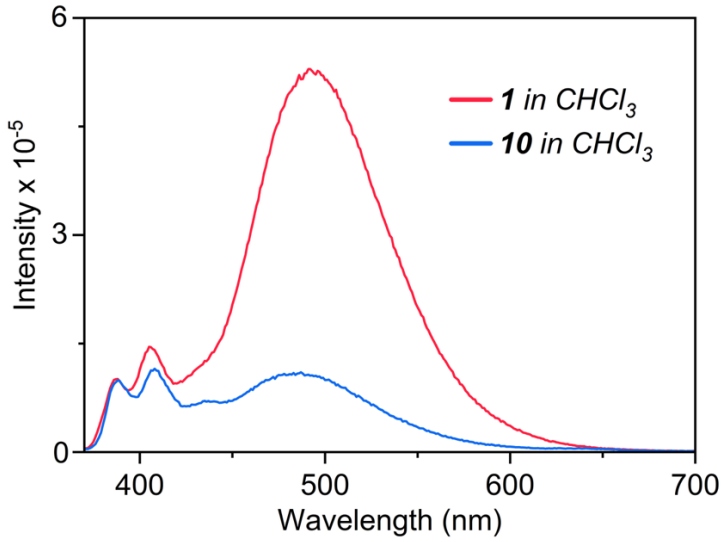

Fig. S10 Fluorescence (λ_{ex}=360 nm) spectra of 6 μM solution of **1** and **10** in chloroform at 298 K. It indicates that the excimer emission in **1** is nearly five times more intense than that of **10**.

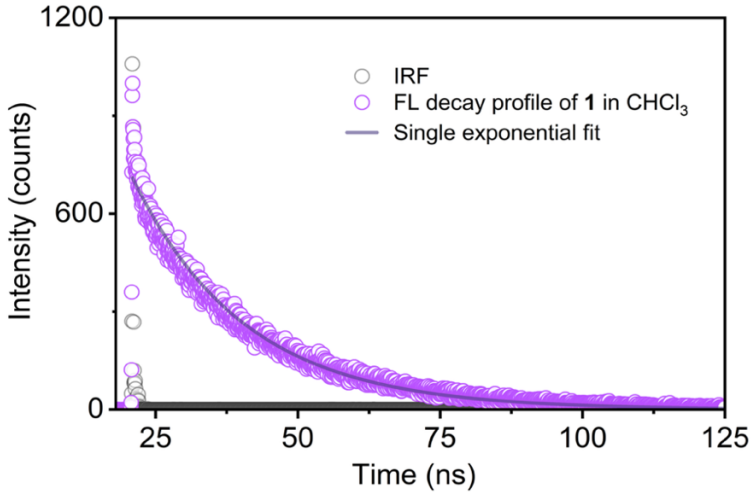

Fig. S11 Fluorescence decay profile of **1** in $CHCl_3$ (λ_{ex} = 375 nm, $\lambda_{monitored}$ = 493 nm, τ = 19. 9 ns).

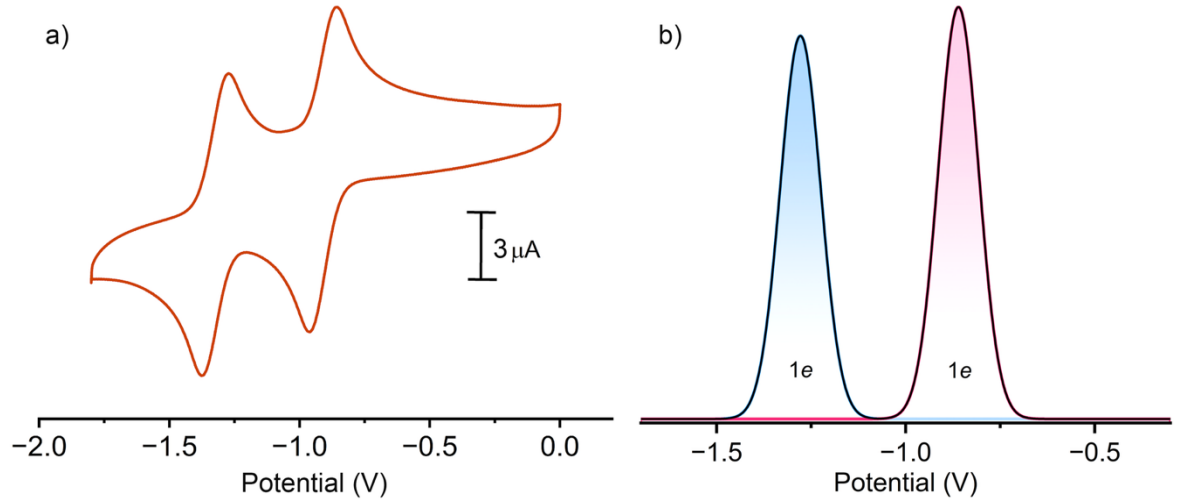

Fig. S12 (a) Cyclic voltammogram (CV) of **NDI-ref** at 0.2 mM concentration. The CV was recorded using degassed anhydrous DCM using 0.1 M NBu_4PF_6 as a supporting electrolyte at room temperature. The $E_{1/2}$ for the first and second reduction are -0.91 V and -1.32 V. (b) Differential pulse voltammogram (DPV) in 10mV step pulse. Each reduction process involves one electron each. Potentials are given against Fc/Fc^+.

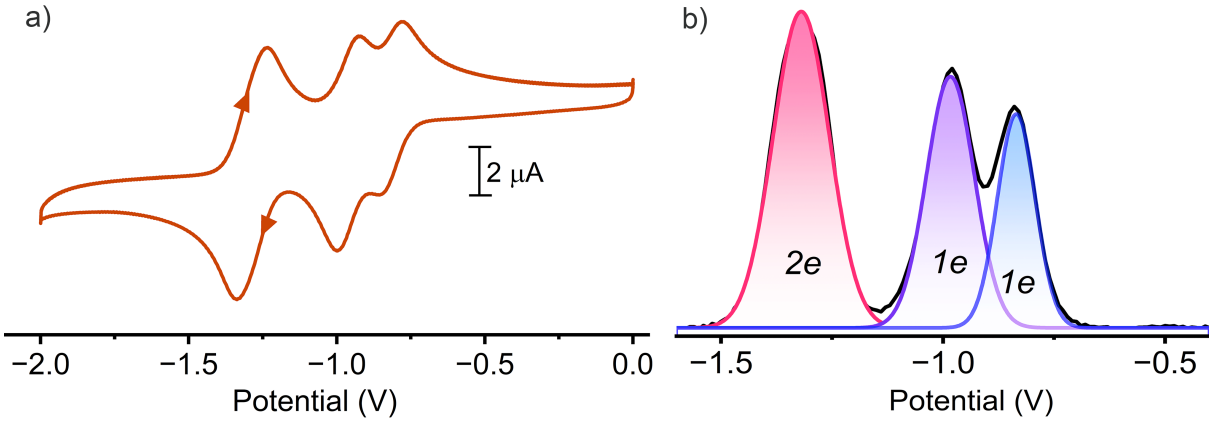

Fig. S13 (a) Cyclic voltammogram (CV) of **10** at 0.2 mM concentration. The CV was recorded in degassed anhydrous DCM using 0.1 M NBu_4PF_6 as a supporting electrolyte at room temperature. The $E_{1/2}$ values against Fc/Fc^+ are -0.85 V, -1.01 V, and -1.28 V. (b) Differential pulse voltammogram (DPV) in 10mV step pulse. The peaks are deconvoluted to quantify the number of electrons involved in each reduction process. Potentials are given against Fc/Fc^+.

Stepwise reduction of NDI units in the oligomer: The sequential reduction behaviour observed in the DPV of the NDI-tetramer **1** suggests a stepwise electron-uptake mechanism. It can be anticipated that the first one-electron reduction at −0.76 V occurs on one of the interior NDI, which can be stabilized by the two adjacent NDI units through donor-acceptor interactions. The second one-electron reduction at −0.89 V is most likely to occur in one of the terminal NDI to have the radical anion far from the previous radical anion at the interior. The third reduction at −0.97 V, involving two electrons, yields a relatively broader voltammogram, which we anticipate corresponds to the reduction of the remaining two NDI moieties. After the uptake of the initial four electrons, **1** forms four radical anions, which later take four more electrons (at -1.31 V) to undergo the second reduction of all NDIs to form an overall 8-electron reduced species. This can be correlated with the following figure.

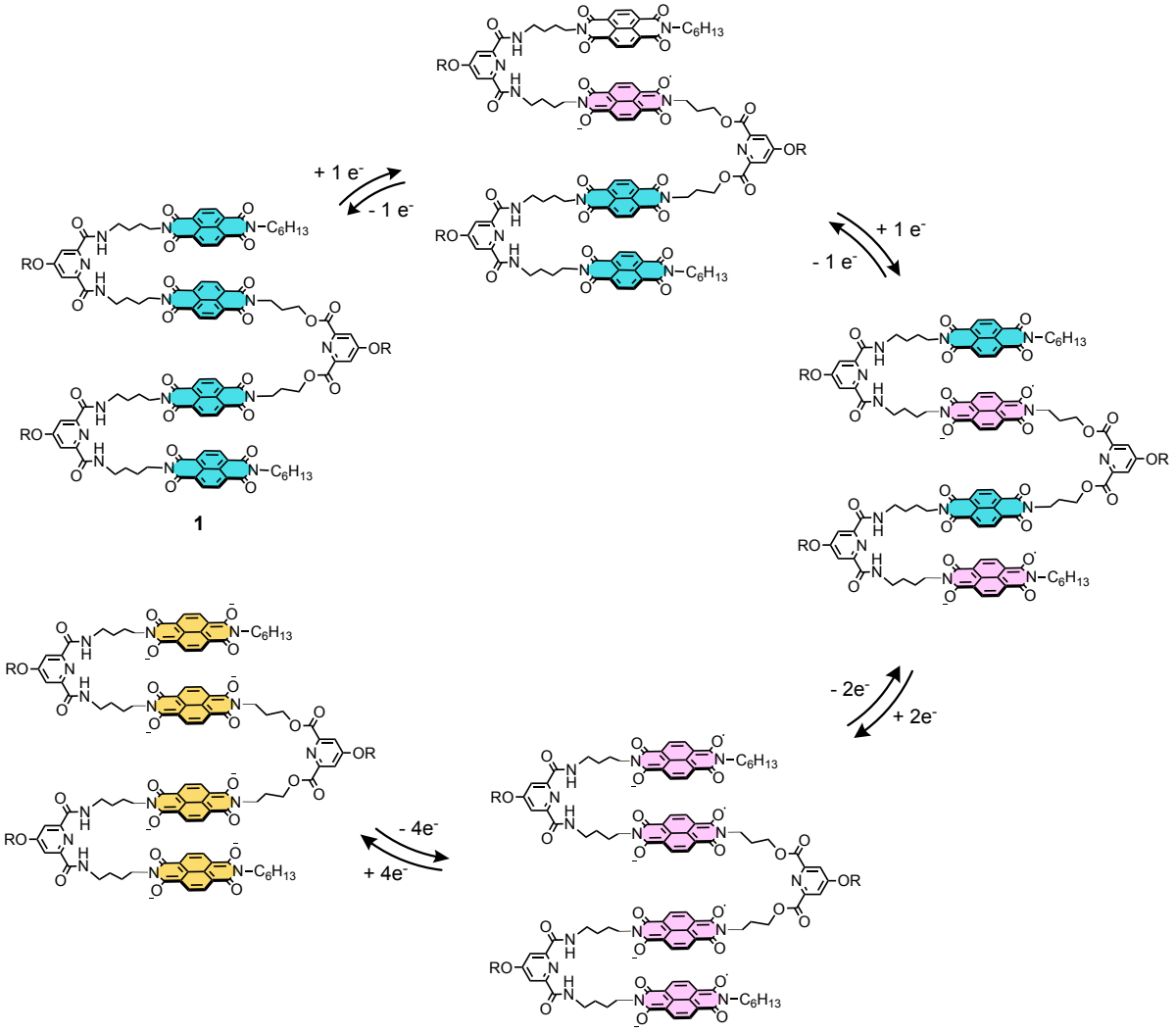

Fig. S14 The proposed stepwise reduction of the NDI units in the oligomer.

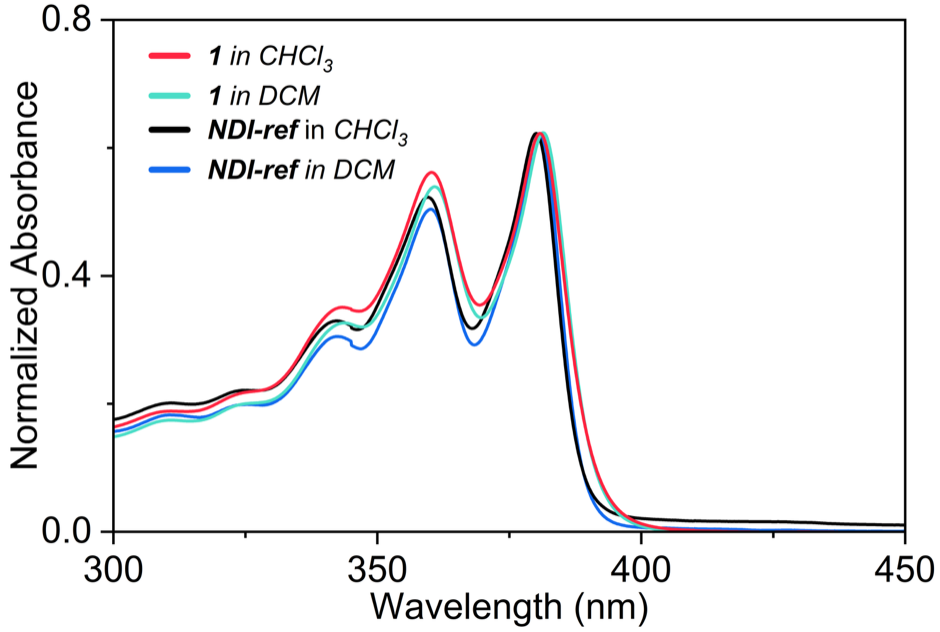

Fig. S15 UV-Vis spectra of **1** and **NDI-ref** in DCM and $CHCl_3$. $A_{0\text{-}0}/A_{0\text{-}1}$ ratio calculated for **1** in DCM is 1.11 and in $CHCl_3$ is 1.16; however, for **NDI-ref**, $A_{0\text{-}0}/A_{0\text{-}1}$ ratio calculated is 1.21 in DCM and 1.2 in $CHCl_3$.

4. Solvent-Dependent Studies

4.1. UV-Visible studies for aliphatic solvents

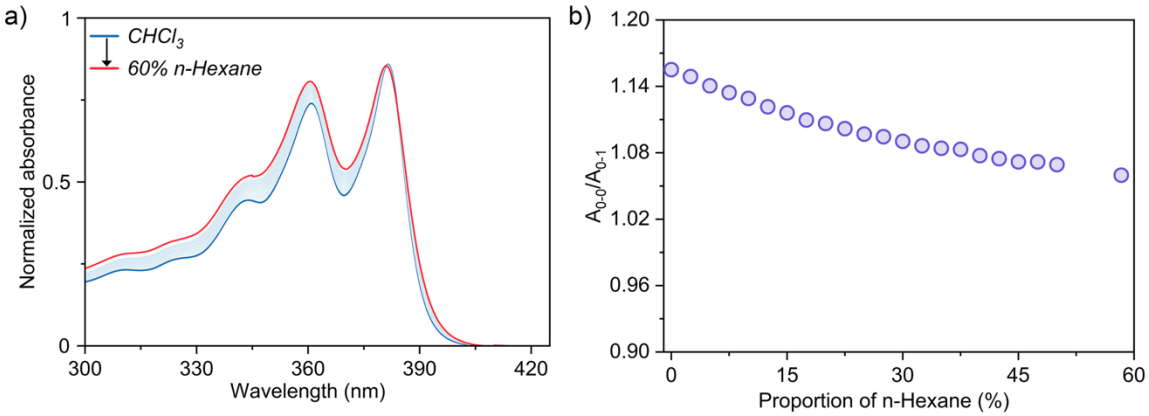

Fig. S16 (a) UV-Visible absorption spectra of **1** (6 μM in $CHCl_3$) with the gradual addition of n-hexane at 298 K. The UV-Vis spectra are normalised at 381 nm. (b) $A_{0\text{-}0}/A_{0\text{-}1}$ plotted against proportion of n-hexane in $CHCl_3$. There is a gradual decrease in $A_{0\text{-}0}/A_{0\text{-}1}$ observed when *n*-hexane is added to 6 μM solution of **1** in $CHCl_3$.

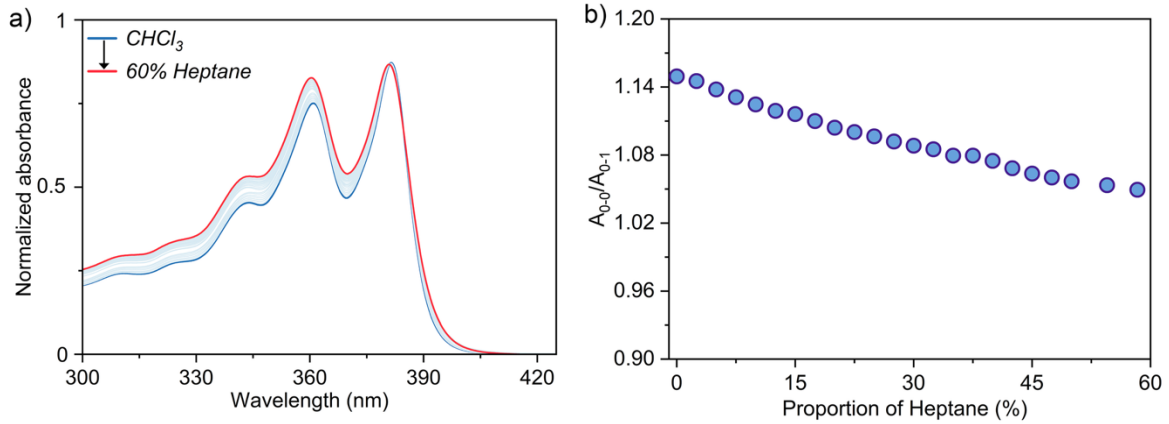

Fig. S17 (a) UV-Visible absorption spectra of **1** (6 μM in $CHCl_3$) with the gradual addition of heptane at 298 K. The UV-Vis spectra are normalised at 381 nm. (b) A_{0-0}/A_{0-1} plotted against proportion of heptane in $CHCl_3$. There is a gradual decrease in A_{0-0}/A_{0-1} observed when heptane is added to 6 μM solution of **1** in $CHCl_3$.

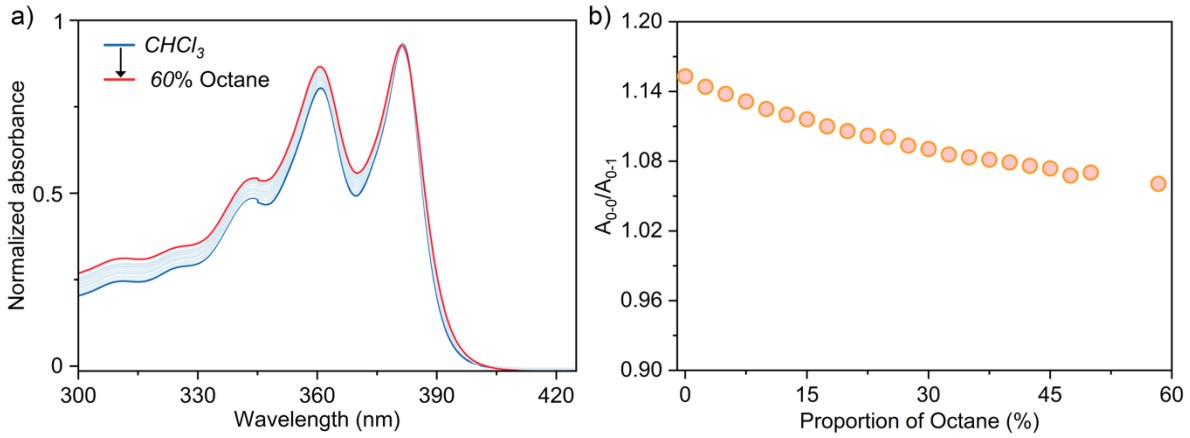

Fig. S18 UV-Visible absorption spectra of **1** (6 μM in $CHCl_3$) with the gradual addition of octane at 298 K. The UV-Vis spectra are normalised at 381 nm. (b) A_{0-0}/A_{0-1} plotted against proportion of octane in $CHCl_3$. There is a gradual decrease in A_{0-0}/A_{0-1} observed when octane is added to 6 μM solution of **1** in $CHCl_3$.

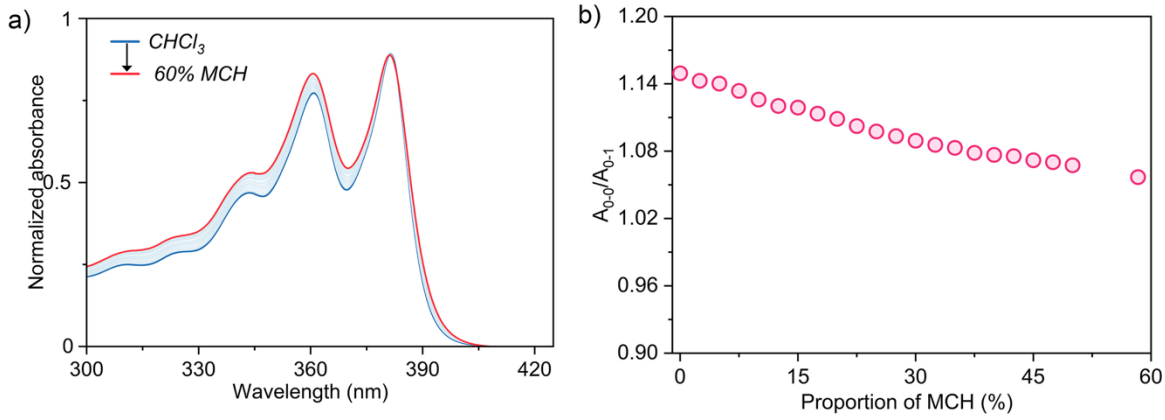

Fig. S19 UV-Visible absorption spectra of **1** (6 μM in $CHCl_3$) with the gradual addition of MCH at 298 K. The UV-Vis spectra are normalised at 381 nm. (b) A_{0-0}/A_{0-1} plotted against proportion of MCH in $CHCl_3$. There is a gradual decrease in A_{0-0}/A_{0-1} observed when MCH is added to 6 μM solution of **1** in $CHCl_3$.

4.2. UV-Visible studies for aromatic solvents

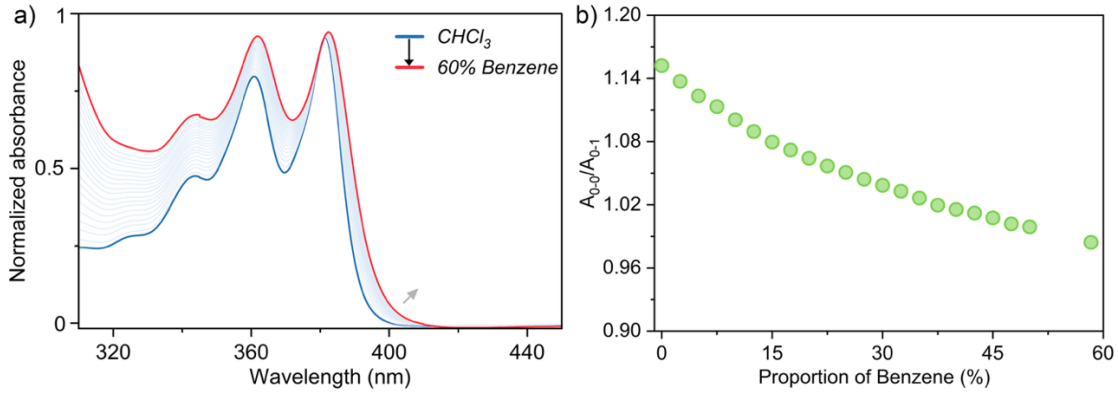

Fig. S20 (a) UV-Visible absorption spectra of **1** (6 µM in $CHCl_3$) with the gradual addition of benzene at 298 K. The UV-Vis spectra are normalised at 381 nm. (b) $A_{0\text{-}0}/A_{0\text{-}1}$ plotted against proportion of benzene in $CHCl_3$. There is a gradual decrease in $A_{0\text{-}0}/A_{0\text{-}1}$ observed when benzene is added to 6 µM solution of **1** in $CHCl_3$.

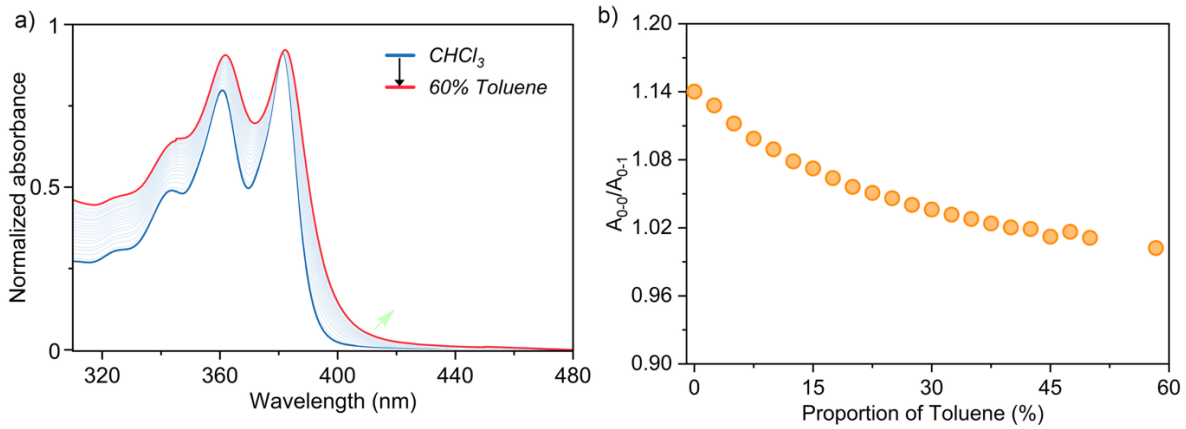

Fig. S21 UV-Visible absorption spectra of **1** (6 µM in $CHCl_3$) with the gradual addition of toluene at 298 K. The UV-Vis spectra are normalised at 381 nm. (b) $A_{0\text{-}0}/A_{0\text{-}1}$ plotted against the proportion of toluene in $CHCl_3$. There is a gradual decrease in $A_{0\text{-}0}/A_{0\text{-}1}$ observed when toluene is added to a 6 µM solution of **1** in $CHCl_3$.

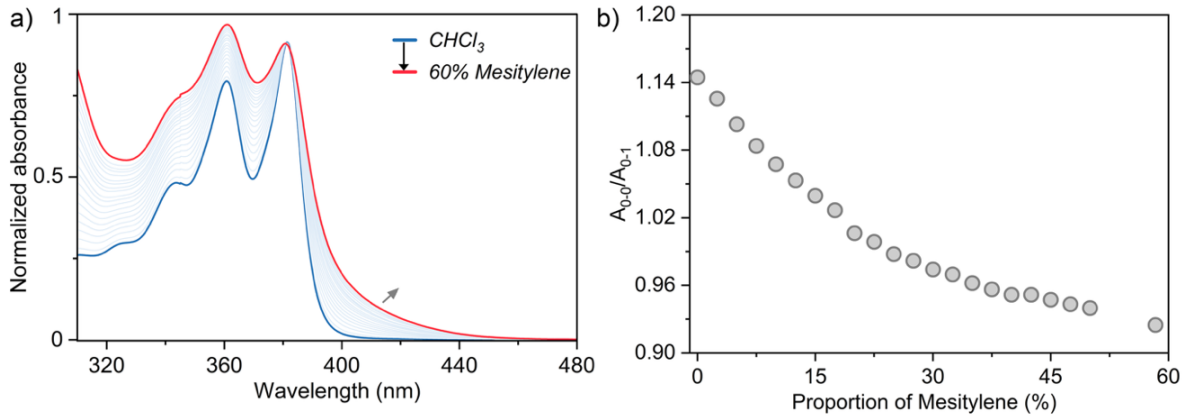

Fig. S22 UV-Visible absorption spectra of **1** (6 µM in $CHCl_3$) with the gradual addition of mesitylene at 298 K. The UV-Vis spectra are normalised at 381 nm. (b) $A_{0\text{-}0}/A_{0\text{-}1}$ plotted against proportion of mesitylene in $CHCl_3$. There is a gradual decrease in $A_{0\text{-}0}/A_{0\text{-}1}$ observed when mesitylene is added to 6 µM solution of **1** in $CHCl_3$.

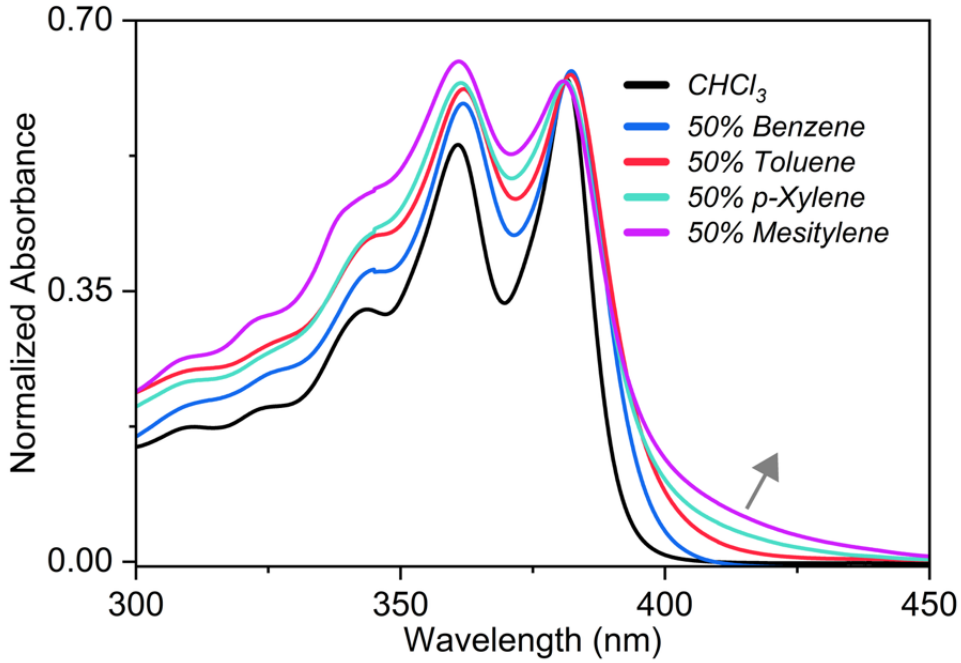

Fig. S23 UV-Visible absorption spectra of **1** (6 μM in $CHCl_3$) after addition of 50% of aromatic solvents at 298 K. The UV-Vis spectra are normalised at 381 nm. The emerging broad absorption band beyond 400 nm is due to the charge-transfer interaction between the NDI and aromatic solvents.

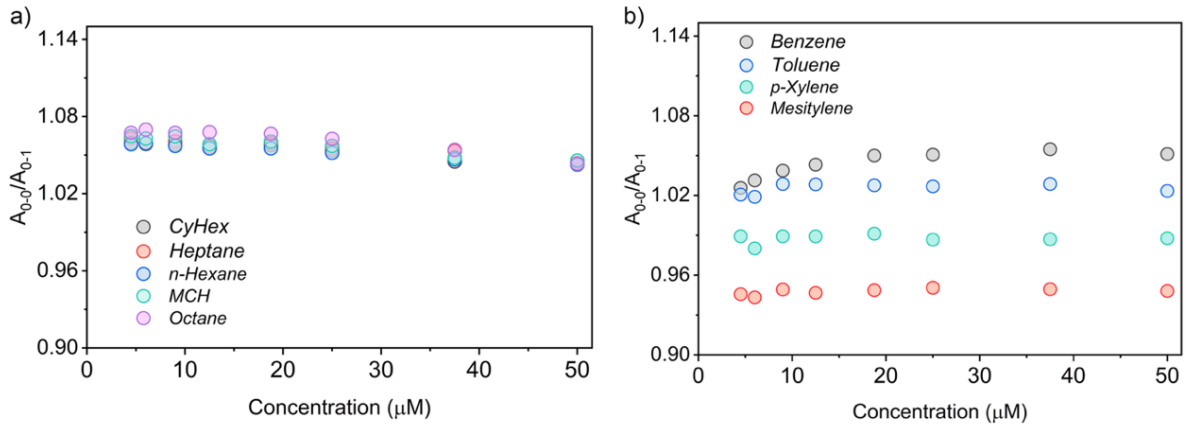

Fig. S24 Variation of $A_{0\text{-}0}/A_{0\text{-}1}$ ratio after addition of 50% of (a) aliphatic solvents (b) aromatic solvents in different concentrations of **1** in $CHCl_3$. A nearly unchanged value indicates an intramolecular phenomenon in this concentration range.

4.3. Fluorescence studies for aliphatic solvents

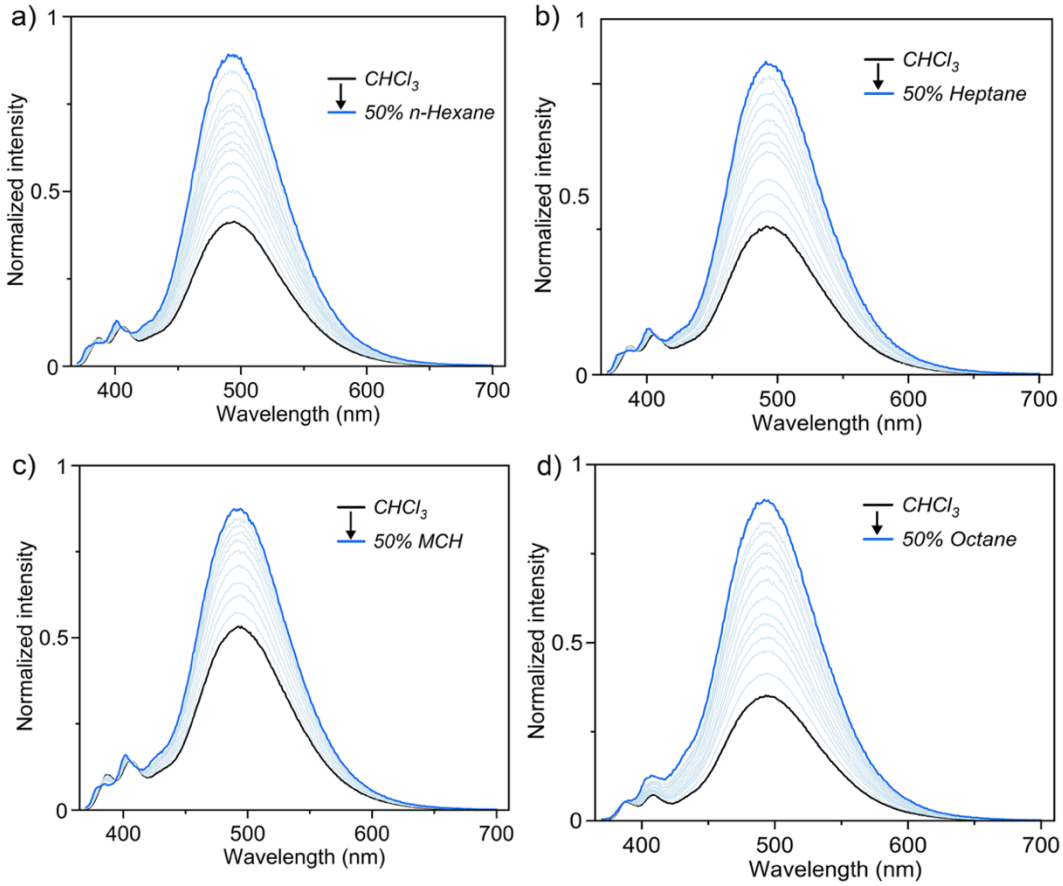

Fig. S25 Fluorescence spectra of **1** (6 μM) with the gradual addition of (a) n-hexane **(**b) heptane (c) MCH (d) octane at 298 K (λ_{ex} = 360 nm). The fluorescence spectra are normalized at 407 nm (monomeric emission).

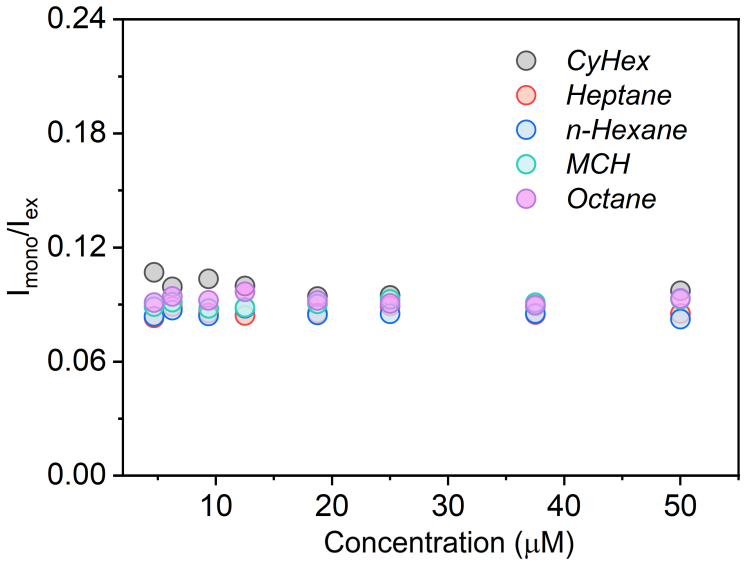

Fig. S26 Variation of monomer (I_{mono}) and excimer (I_{ex}) fluorescence intensity ratio after addition of 50% of aliphatic solvents in different concentrations of **1** in $CHCl_3$. A nearly constant variation indicates an intramolecular folding phenomenon in the excimer emission in this concentration range.

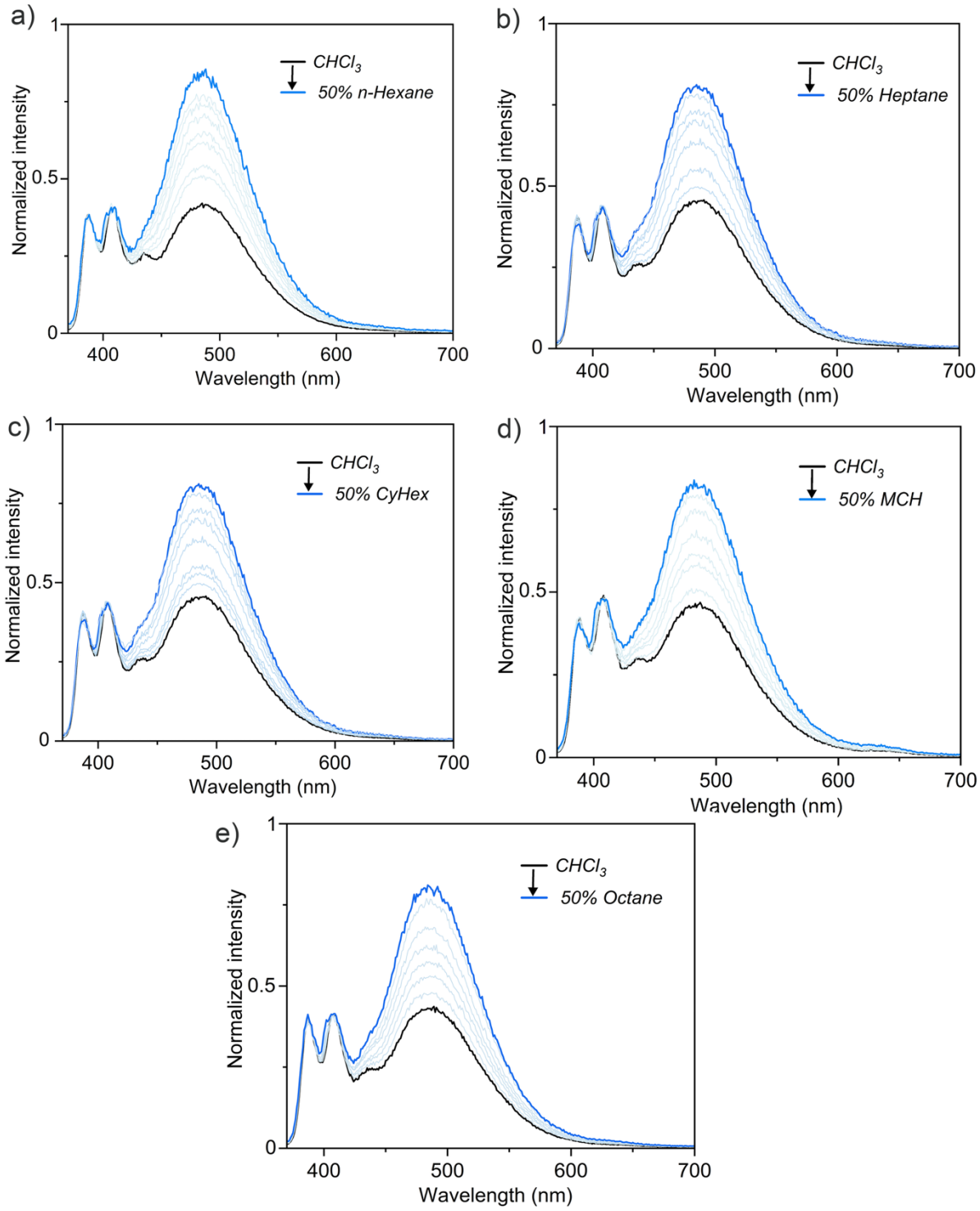

Fig. S27 Fluorescence spectra of **10** (6 μM) with the gradual addition of (a) n-hexane (b) heptane (c) CyHex, (d) MCH, and (e) octane at 298 K (λ_{ex} = 360 nm). The fluorescence spectra are normalized at 407 nm (monomeric emission).

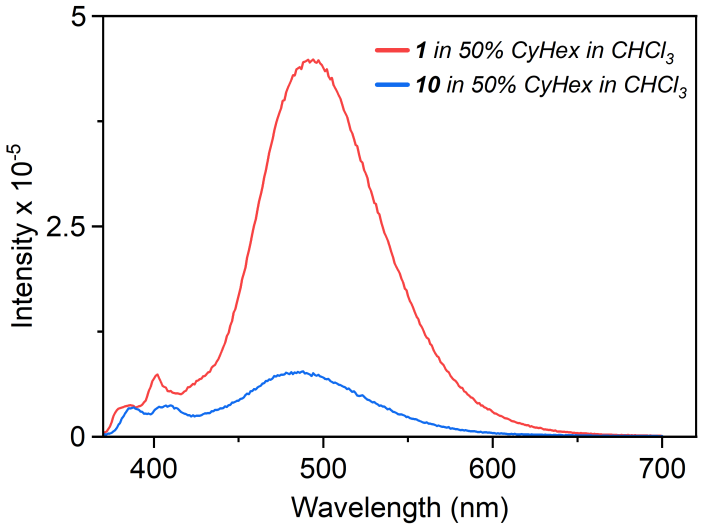

Fig. 28 Comparison of fluorescence (λ_{ex}=360 nm) behavior of 3 μM solution of **1** and **10** after addition of 50% cyclohexane in chloroform at 298 K. It indicates that the excimer emission in **1** is nearly six times more intense than that of **10**.

4.4. Fluorescence studies for aromatic solvents

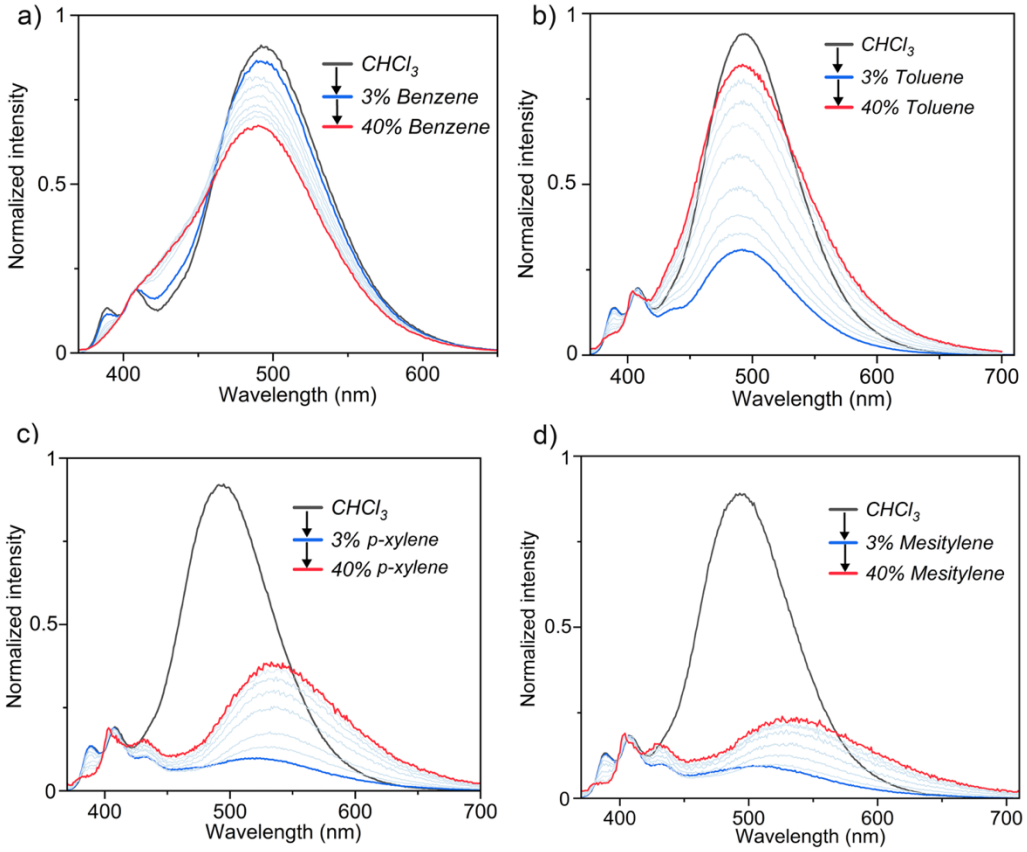

Fig. S29 Fluorescence spectra of **1** (6 μM) with the gradual addition of (a) benzene (b) toluene (c) *p*-xylene (d) mesitylene at 298 K (λ_{ex} = 360 nm). The addition of benzene, toluene, p-xylene, mesitylene results in a broad CT emission band at 495 nm, 500 nm, 536 nm and 540 nm respectively. The fluorescence spectra are normalized at 407 nm (monomeric emission).

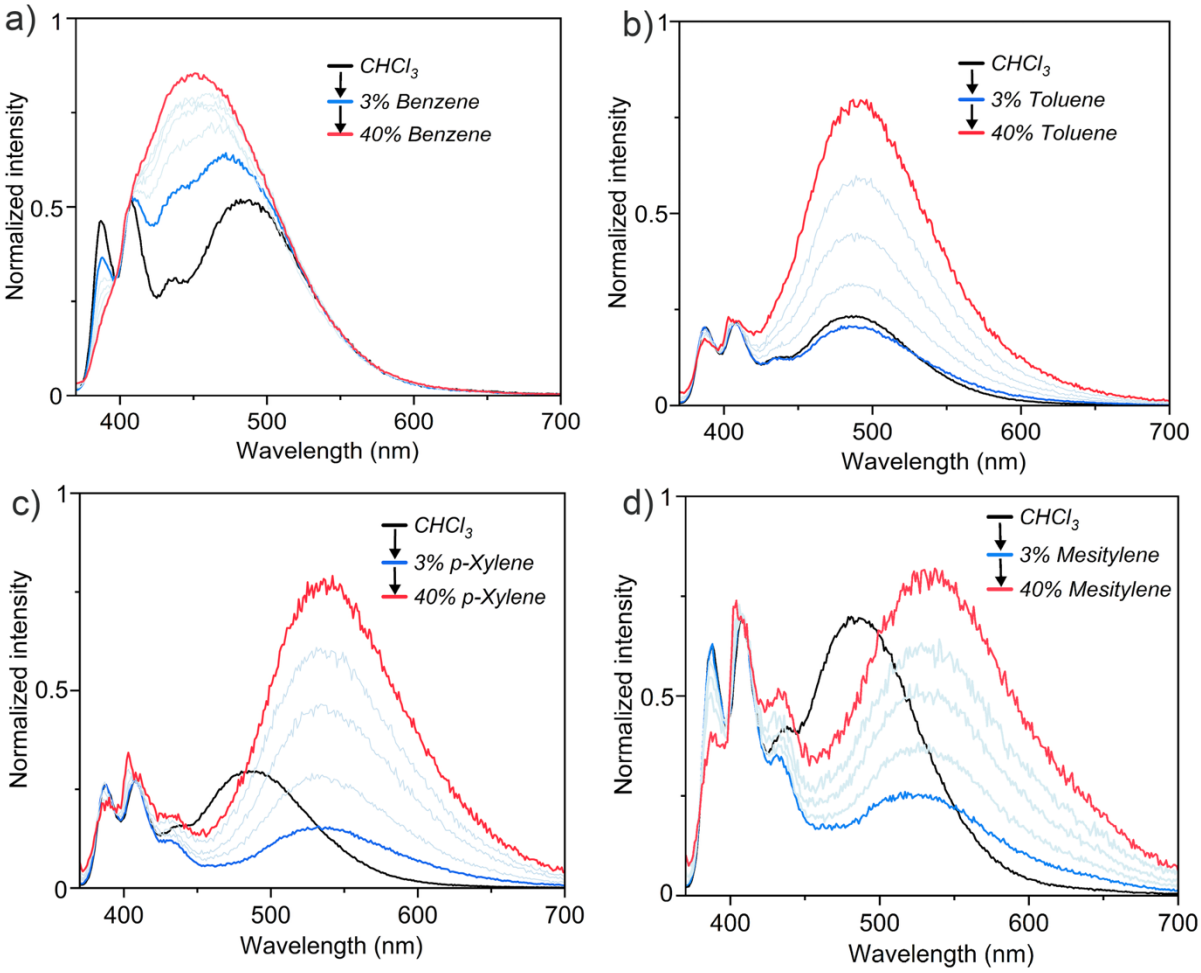

Fig. S30 Fluorescence spectra of **10** (6 μM) with the gradual addition of (a) benzene (b) toluene (c) *p*-xylene (d) mesitylene at 298 K (λ_{ex} = 360 nm). The addition of benzene, toluene, p-xylene, and mesitylene results in a broad CT emission band at 473 nm, 492 nm, 539 nm, and 542 nm, respectively. The fluorescence spectra are normalized at 407 nm (monomeric emission).

4.5. Lifetime Measurements

Aliphatic solvents

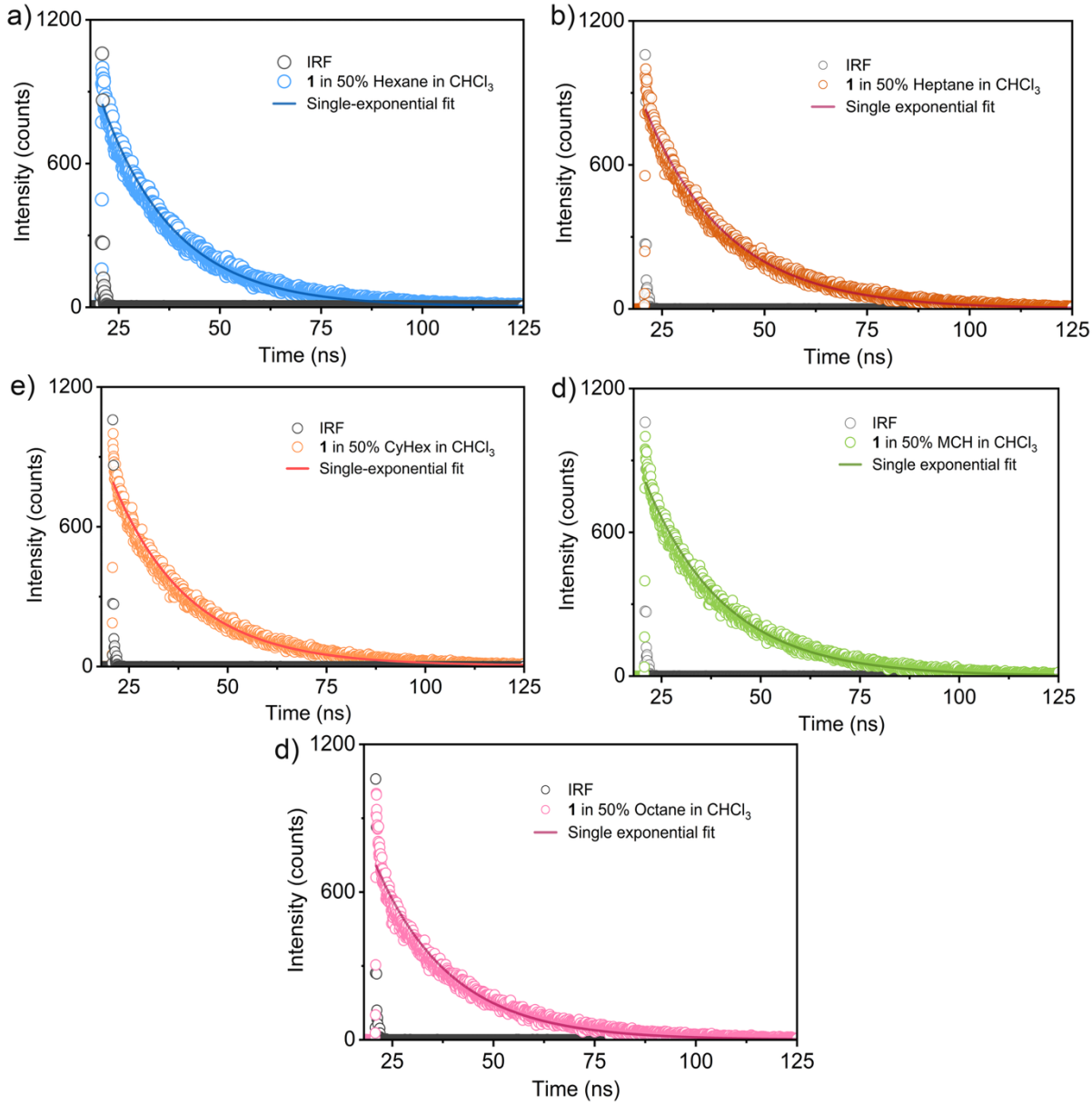

Fig. S31 Fluorescence decay profiles of **1** after addition of (a) 50% n-hexane in $CHCl_3$ (λ_{ex} = 375 nm, $\lambda_{monitored}$ = 493 nm, τ = 18.4 ns), (b) 50% heptane in $CHCl_3$ (λ_{ex} = 375 nm, $\lambda_{monitored}$ = 493 nm, τ = 20.1 ns), (c) 50% cyclohexane in $CHCl_3$ (λ_{ex} = 375 nm, $\lambda_{monitored}$ = 493 nm, τ = 19.5 ns), (d) 50% MCH in $CHCl_3$ (λ_{ex} = 375 nm, $\lambda_{monitored}$ = 493 nm, τ = 19.5 ns), and (e) 50% octane in $CHCl_3$ (λ_{ex} = 375 nm, $\lambda_{monitored}$ = 493 nm, τ = 20.1 ns). The fluorescence decays are fitted with a single exponential in every solvent.

Aromatic solvents

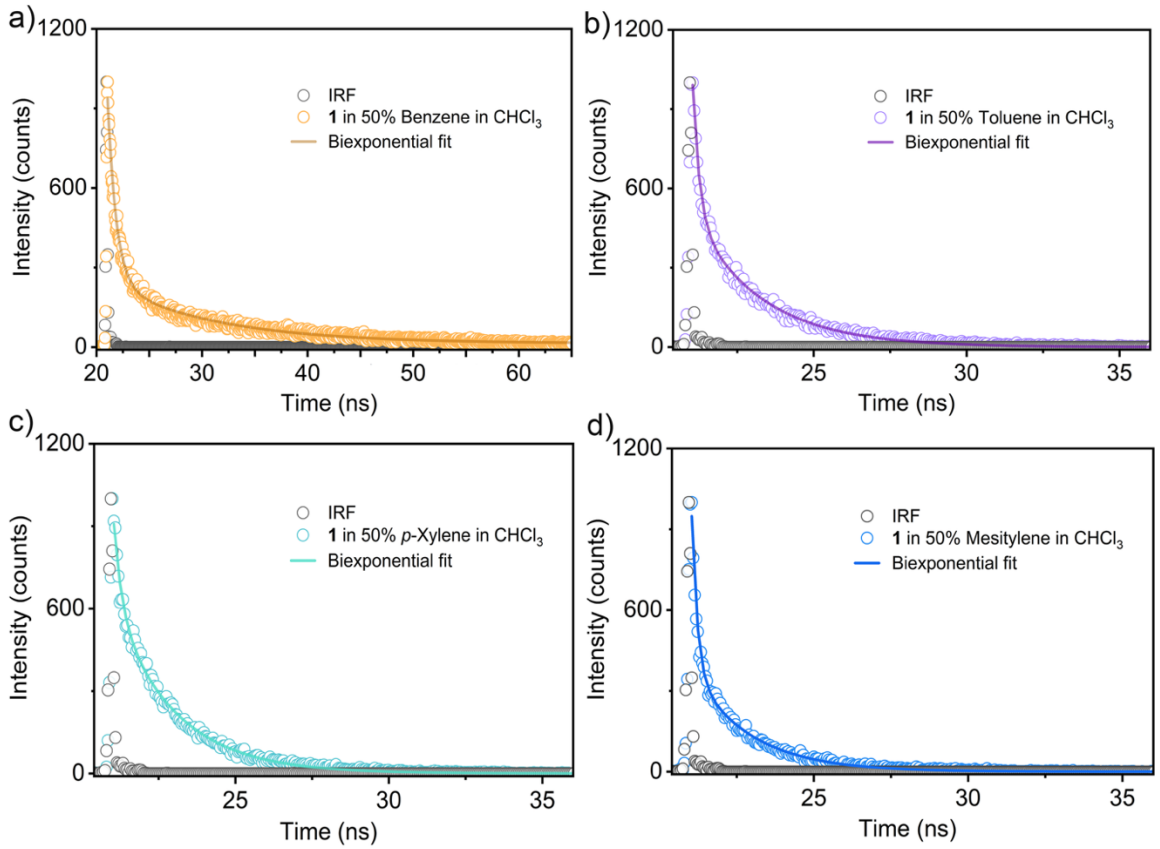

Fig. S32 Fluorescence decay profiles of **1** after addition of (a) 50% benzene in $CHCl_3$ (λ_{ex} = 375 nm, $\lambda_{monitored}$ = 495 nm, τ_{avg} = 0.8 ns, (b) 50% toluene in $CHCl_3$ (λ_{ex} = 375 nm, $\lambda_{monitored}$ = 500 nm, τ_{avg} = 0.2 ns), (c) 50% p-xylene in $CHCl_3$ (λ_{ex} = 375 nm, $\lambda_{monitored}$ = 536 nm, τ_{avg} = 0.2 ns) and (d) 50% mesitylene in $CHCl_3$ (λ_{ex} = 375 nm, $\lambda_{monitored}$ = 540 nm, τ_{avg} = 0.2 ns). The fluorescence decays are fitted with a biexponential in every solvent.

Table 1. The lifetime of the emission band after the addition of 50% aliphatic and aromatic solvents in $CHCl_3$. The sample was excited at 375 nm and monitored at the emission maxima given below. The fluorescence decay for aliphatic solvents was fitted using a single exponential, and for aromatic solvents it was fitted using a biexponential function. In that case, an average lifetime is given.

Addition of 50% solvents	λ_{em}	Lifetime (τ)
n-hexane	493 nm	18.4 ns
Heptane	493 nm	20.1 ns
Octane	493 nm	19.5 ns
Cyclohexane	493 nm	19.5 ns
Methyl cyclohexane	493 nm	20.1 ns
Benzene	495 nm	0.8 ns
Toluene	500 nm	0.2 ns
p-xylene	536 nm	0.2 ns
Mesitylene	540 nm	0.2 ns

5. NMR of the synthesized compounds

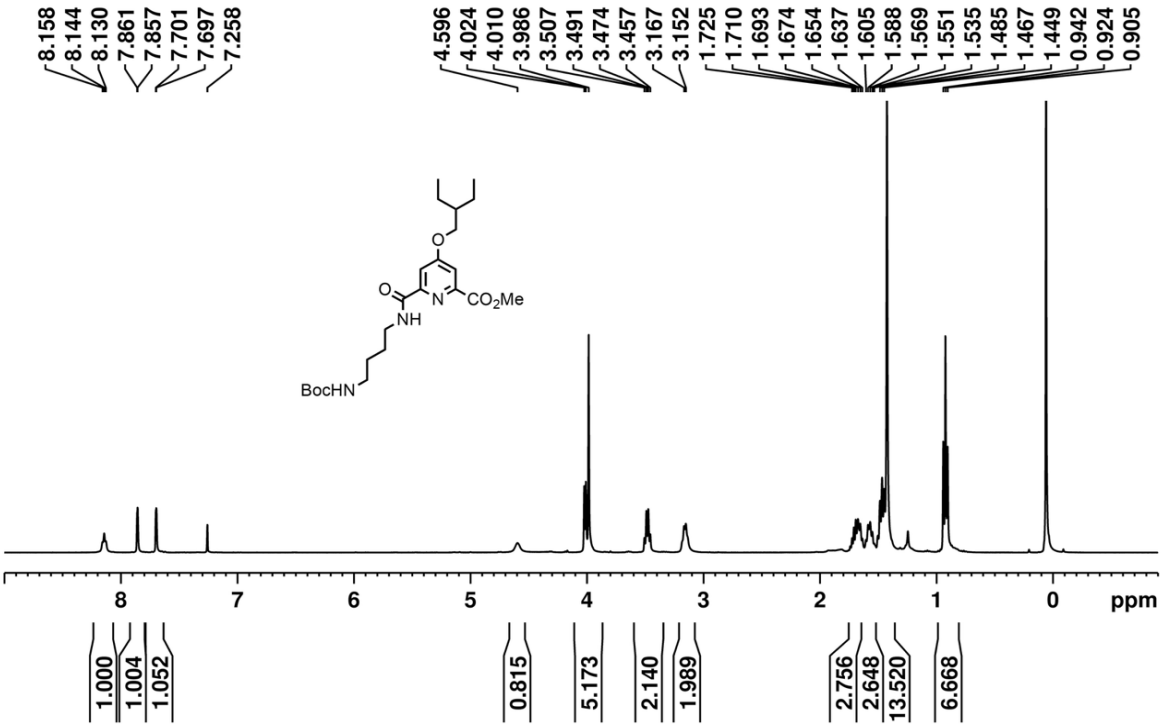

400 MHz, ^{1}H NMR of **3** in $CDCl_3$ at 298 K.

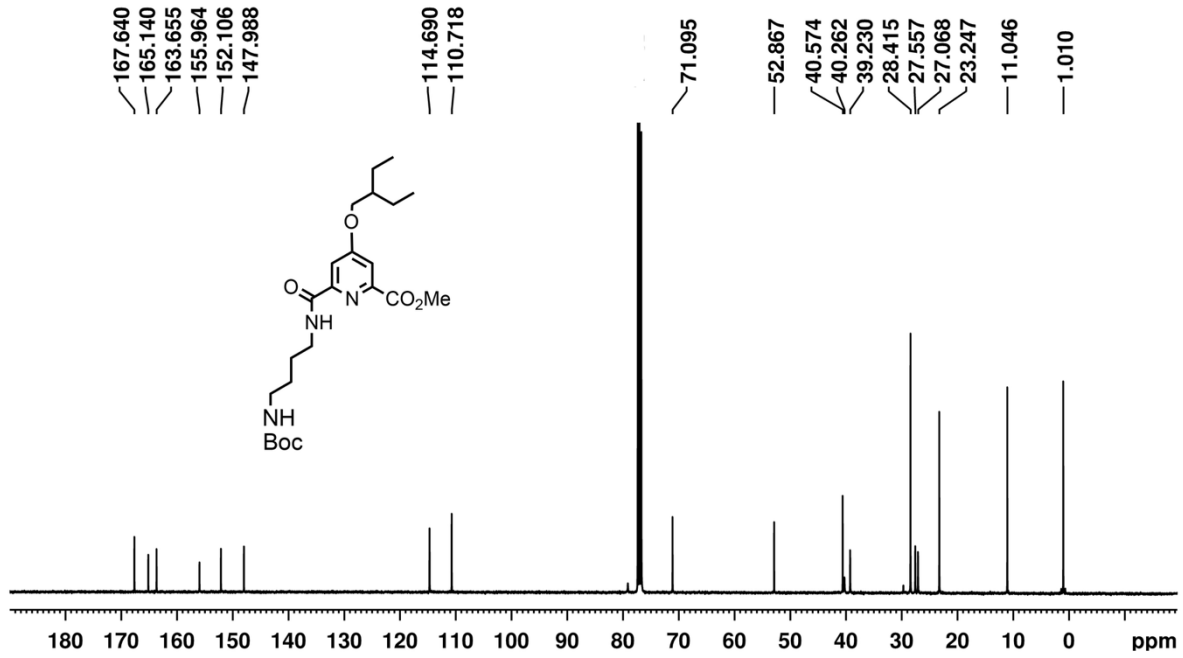

100 MHz, $^{13}C\{1H\}$ NMR of **3** in $CDCl_3$ at 298 K.

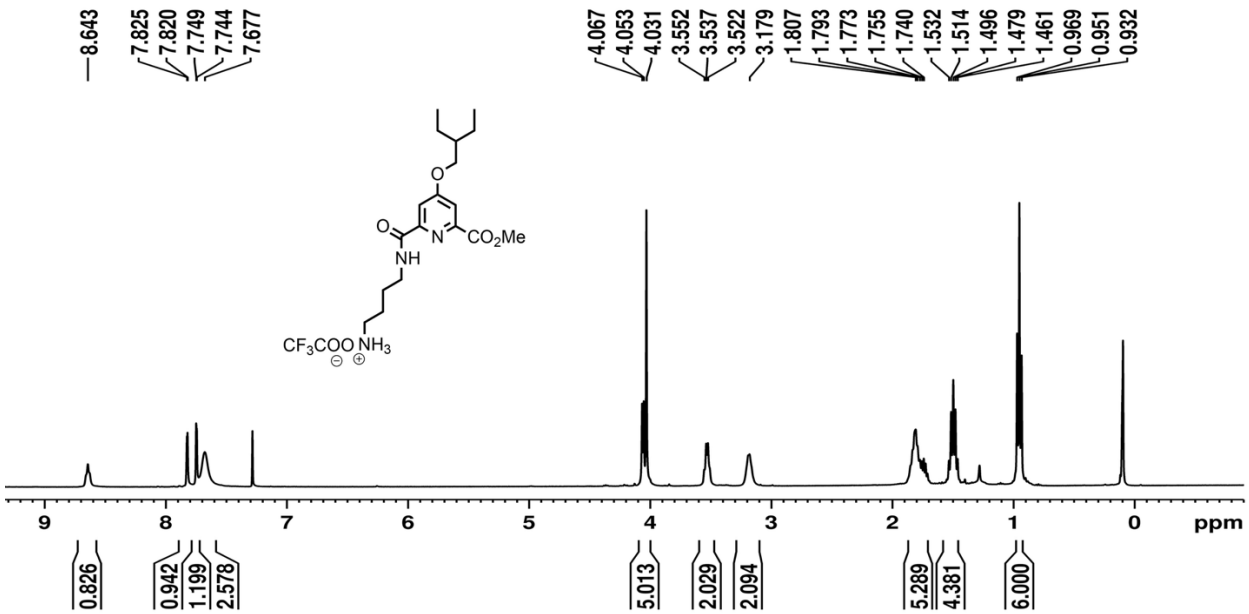

400 MHz, ^{1}H NMR of **4** in $CDCl_3$ at 298 K.

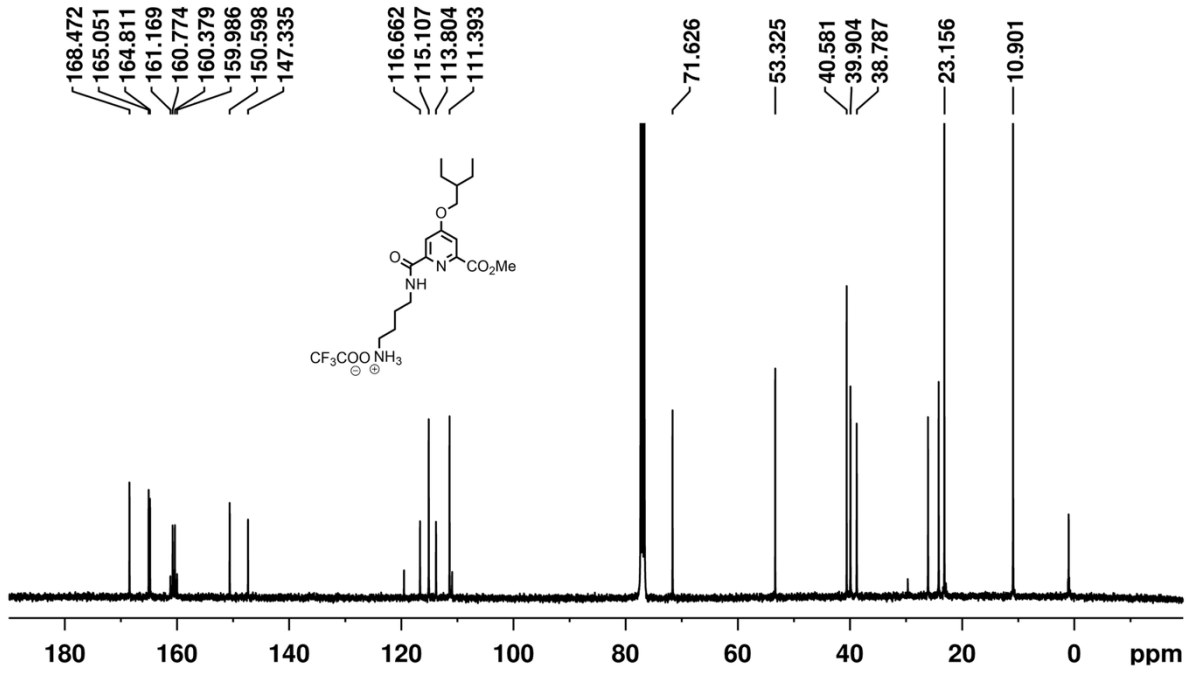

100 MHz, $^{13}C\{1H\}$ NMR of **4** in $CDCl_3$ at 298 K.

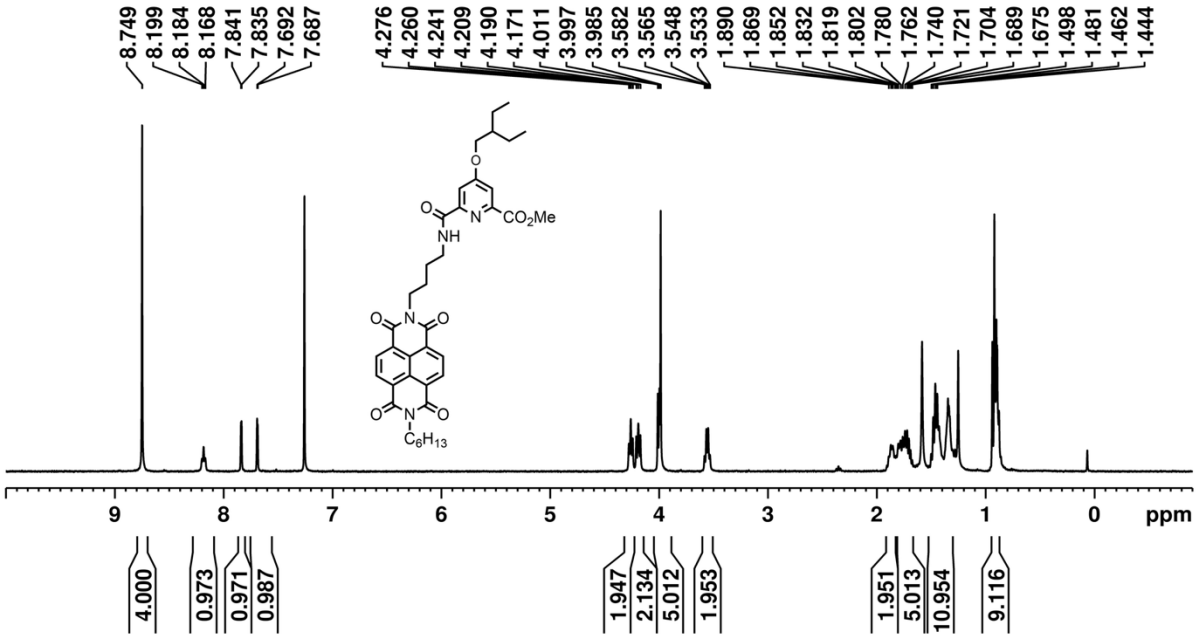

400 MHz, ^{1}H NMR of **6** in $CDCl_3$ at 298 K.

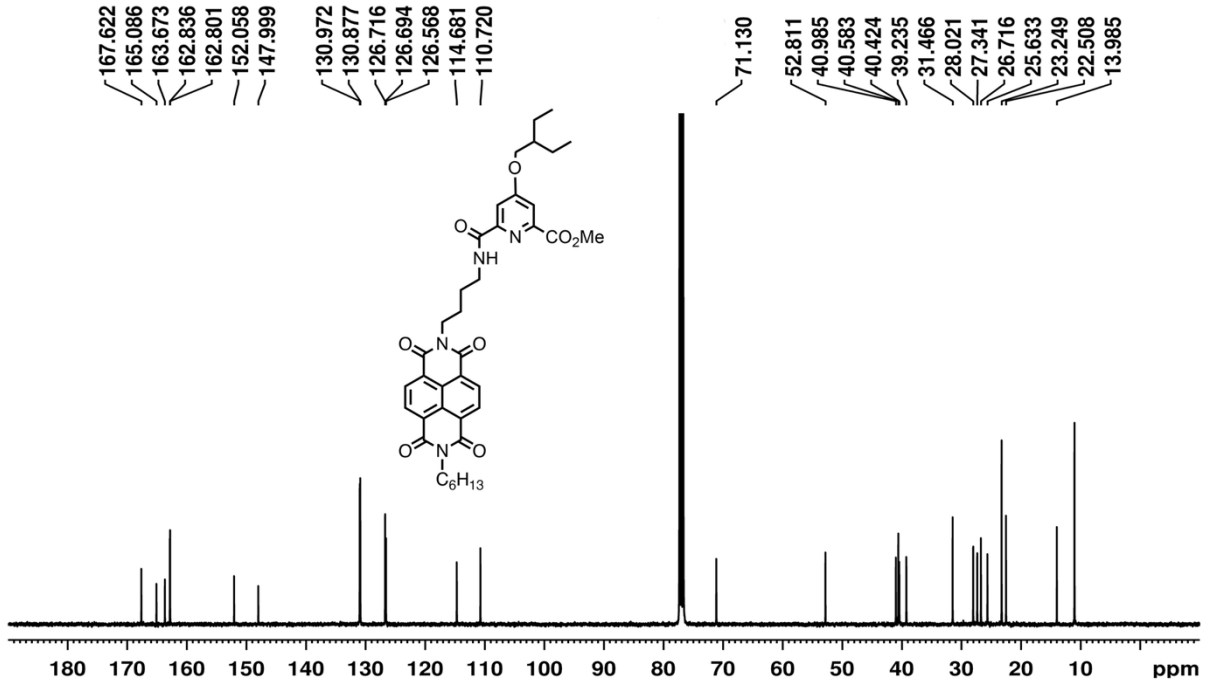

100 MHz, $^{13}C\{1H\}$ NMR of **6** in $CDCl_3$ at 298 K.

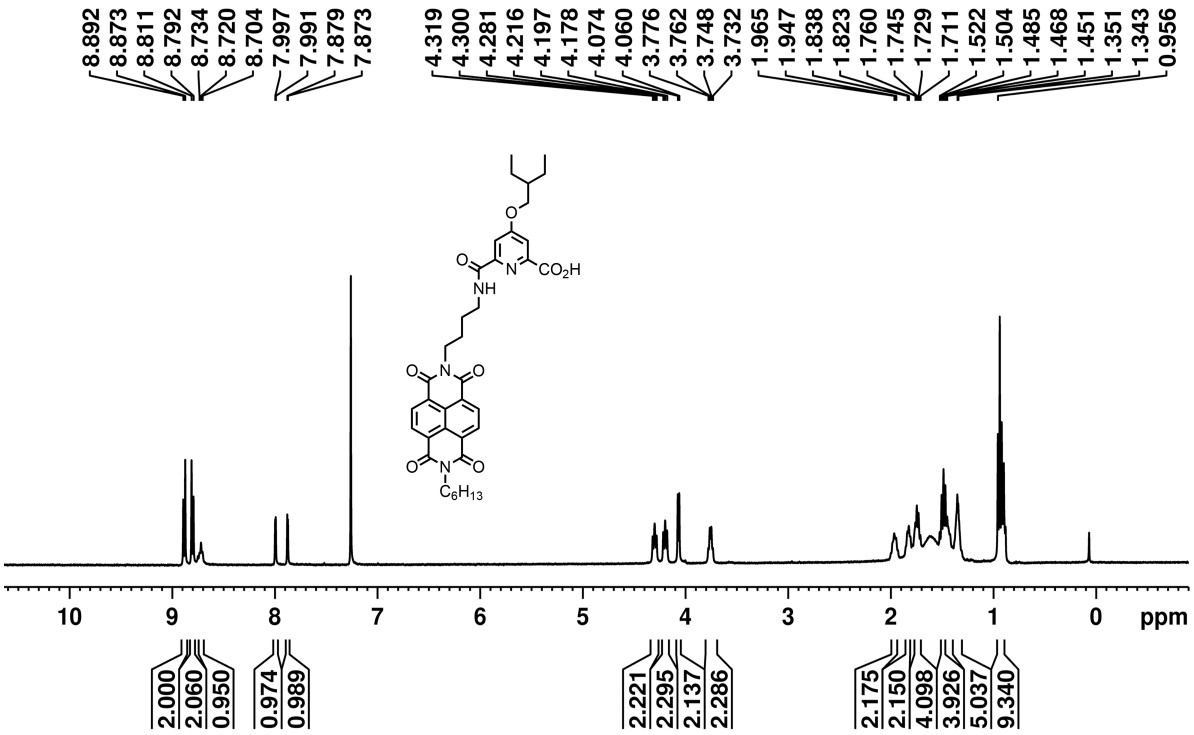

400 MHz, ^{1}H NMR of **7** in $CDCl_3$ at 298 K.

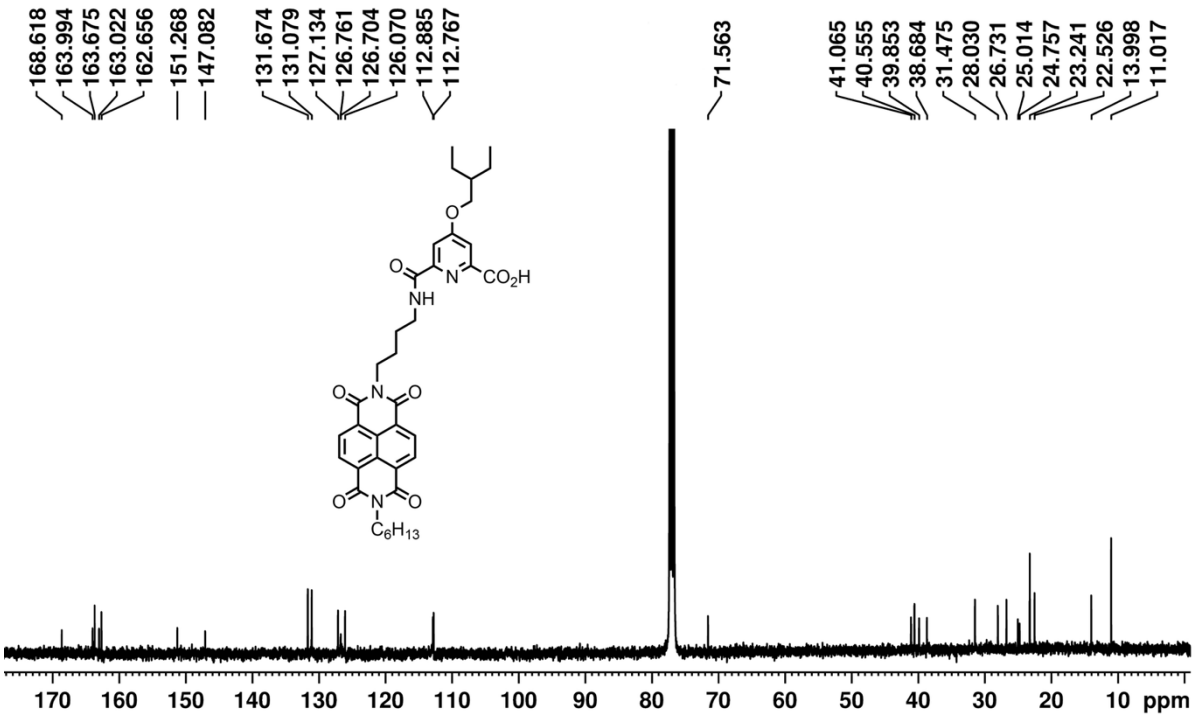

100 MHz, ^{13}C{1H} NMR of **7** in $CDCl_3$ at 298 K.

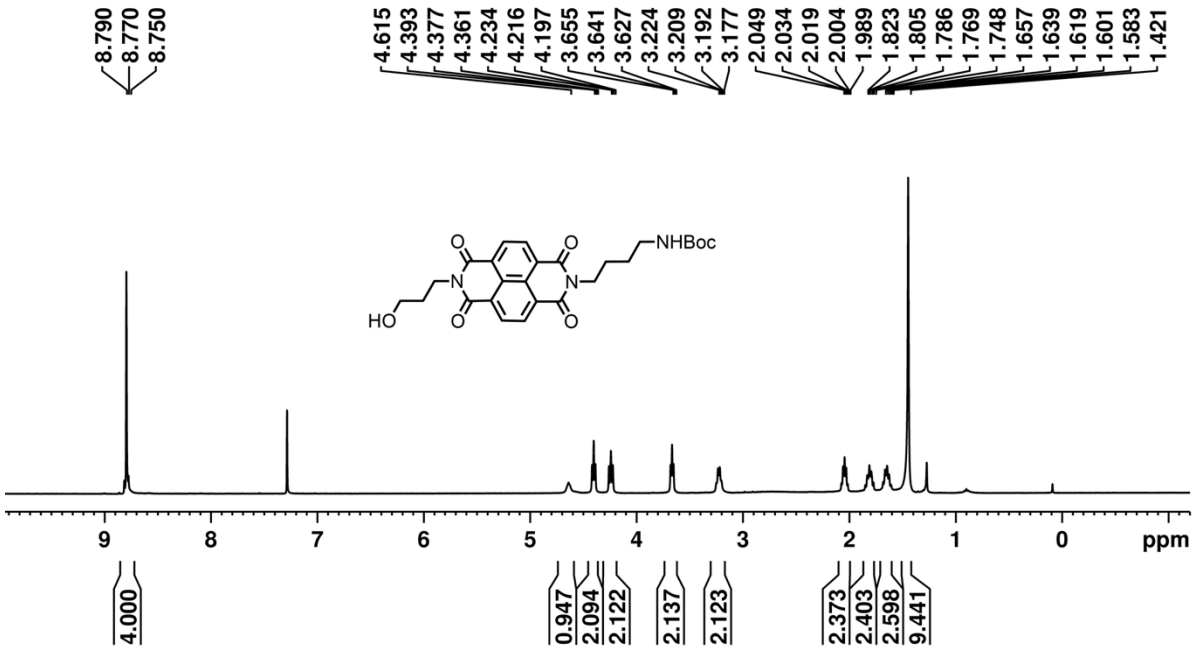

400 MHz, ^{1}H NMR of **9** in $CDCl_3$ at 298 K.

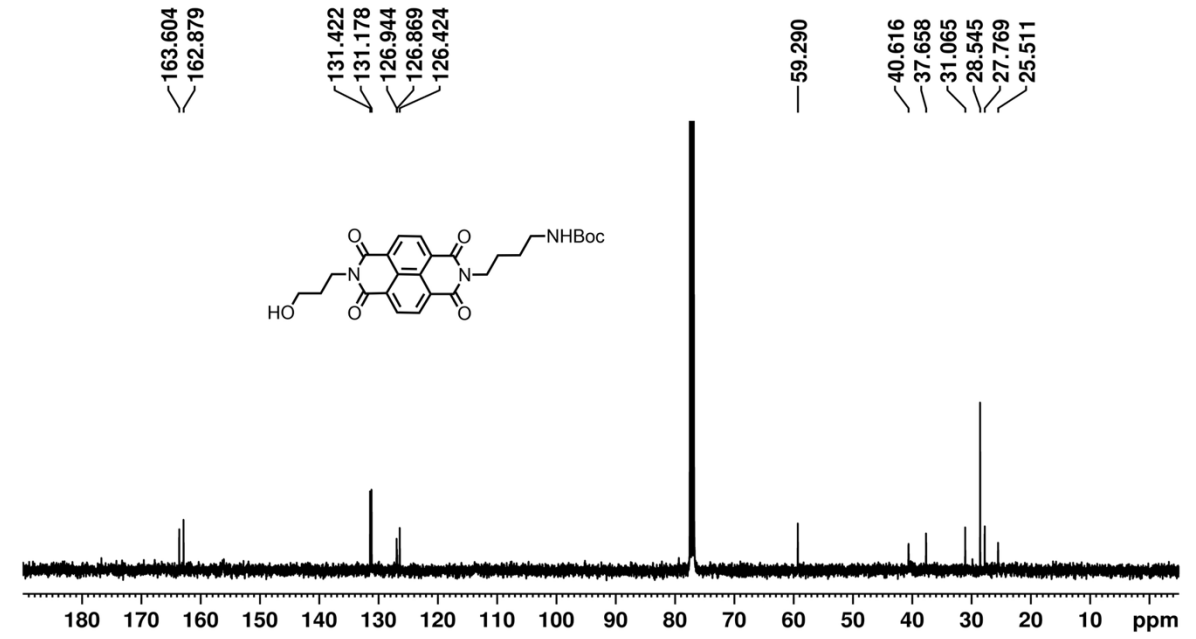

100 MHz, $^{13}C\{1H\}$ NMR of **9** in $CDCl_3$ at 298 K.

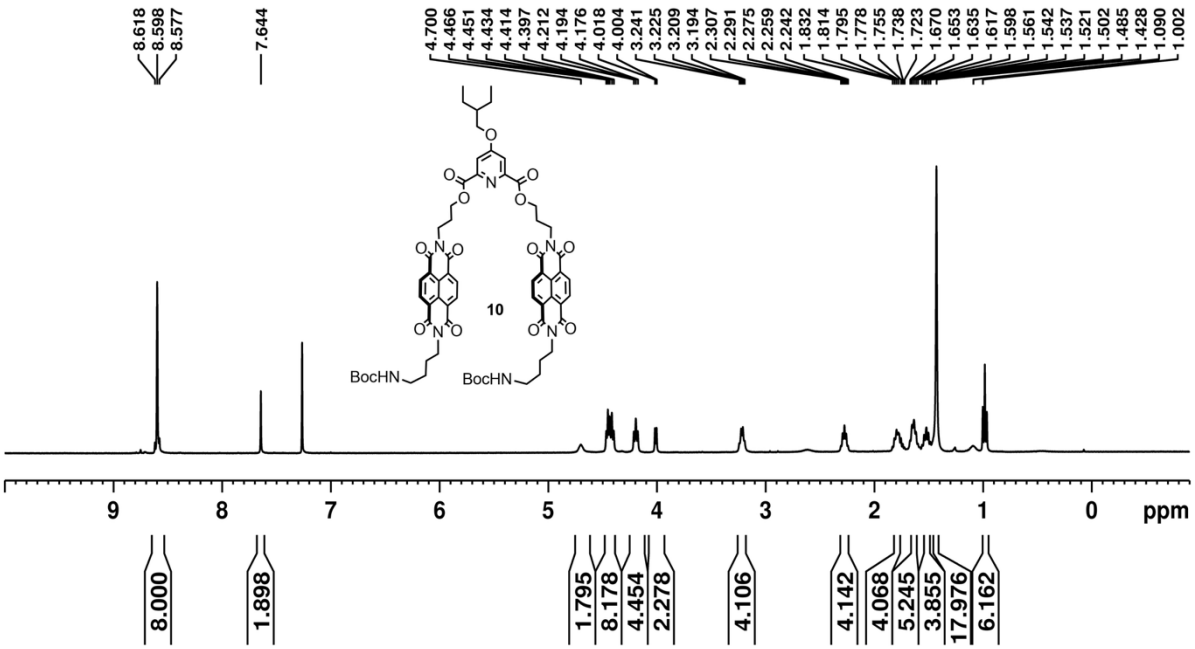

400 MHz, ^{1}H NMR of **10** in $CDCl_3$ at 298 K.

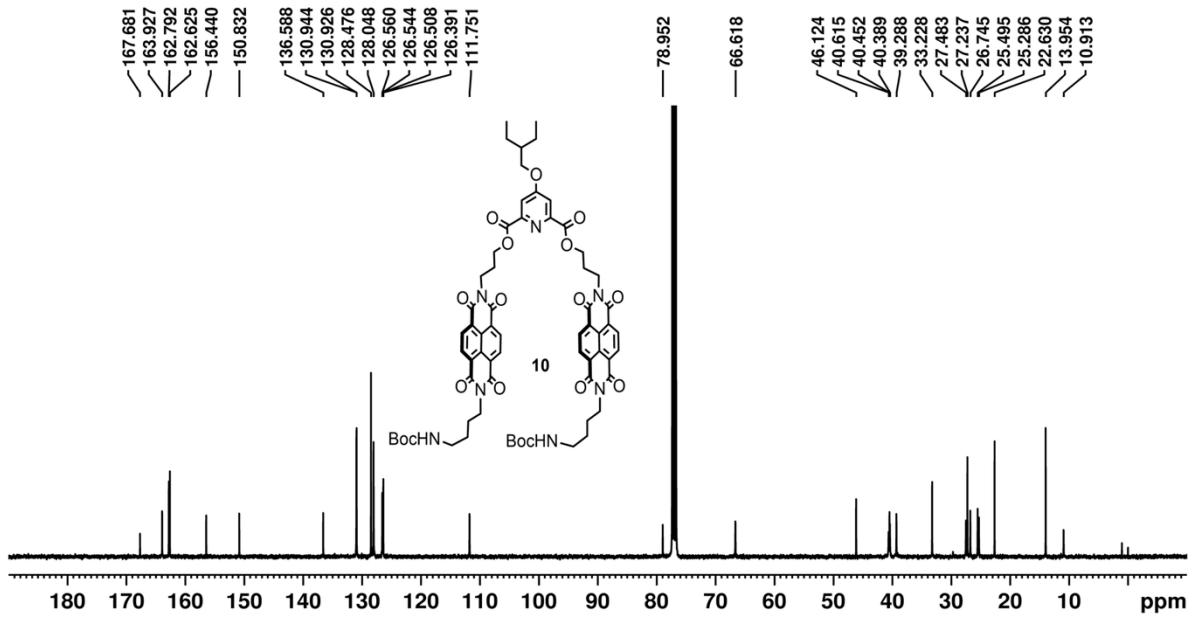

100 MHz, ^{13}C{1H} NMR of **10** in $CDCl_3$ at 298 K.

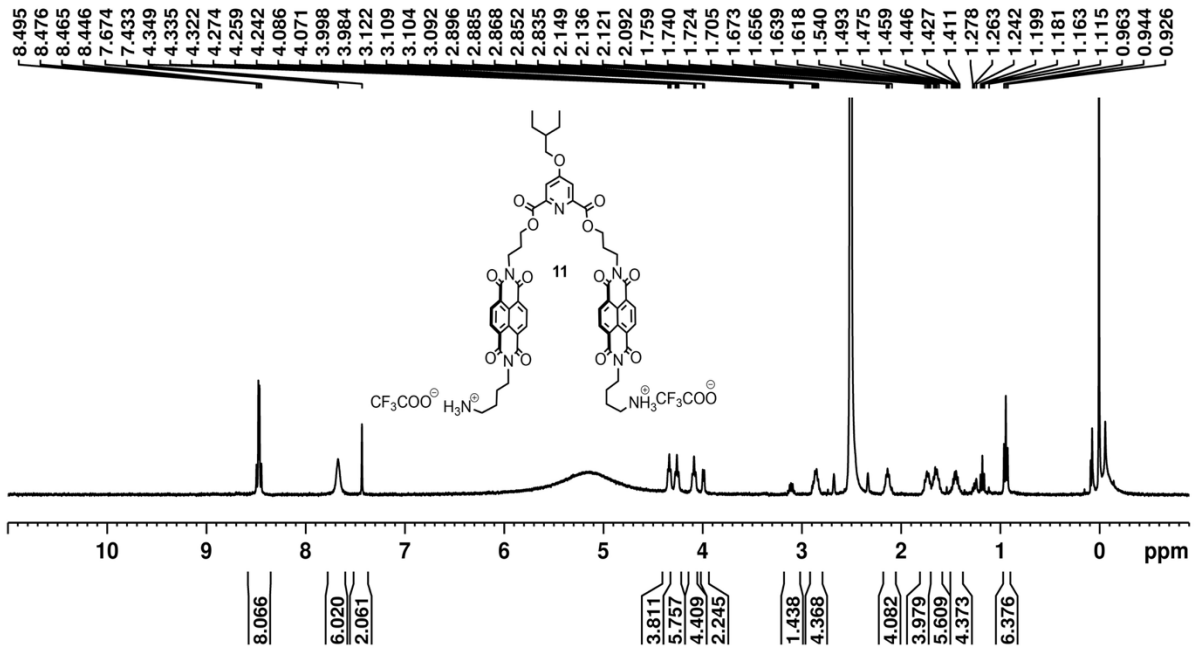

400 MHz, ^{1}H NMR of **11** in $CDCl_3$ at 298 K.

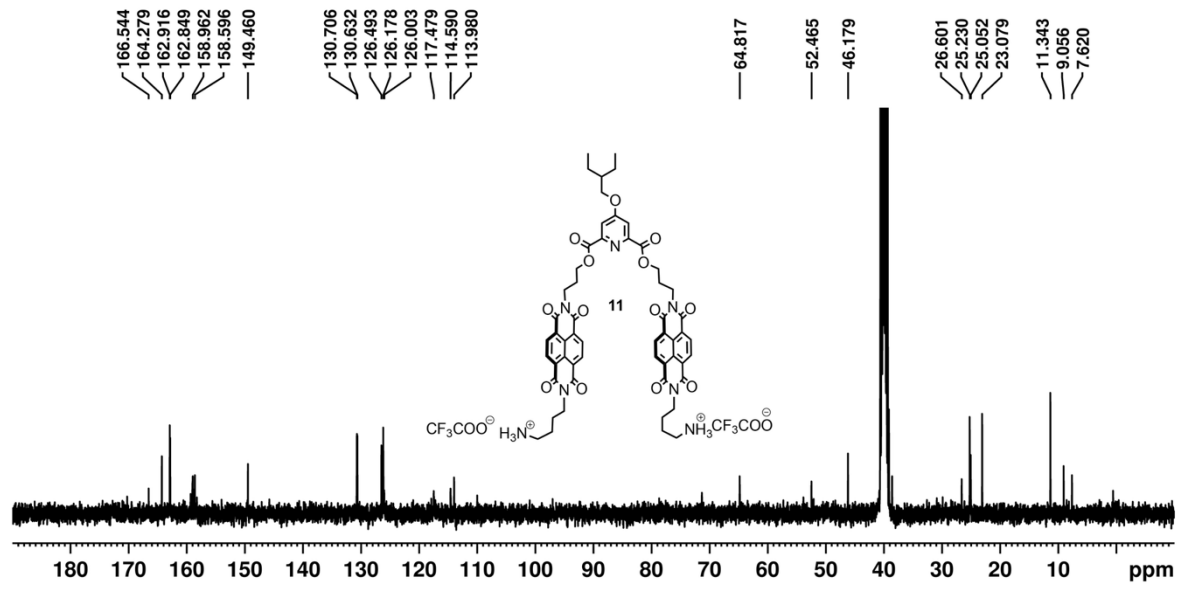

100 MHz, $^{13}C\{1H\}$ NMR of **11** in $CDCl_3$ at 298 K.

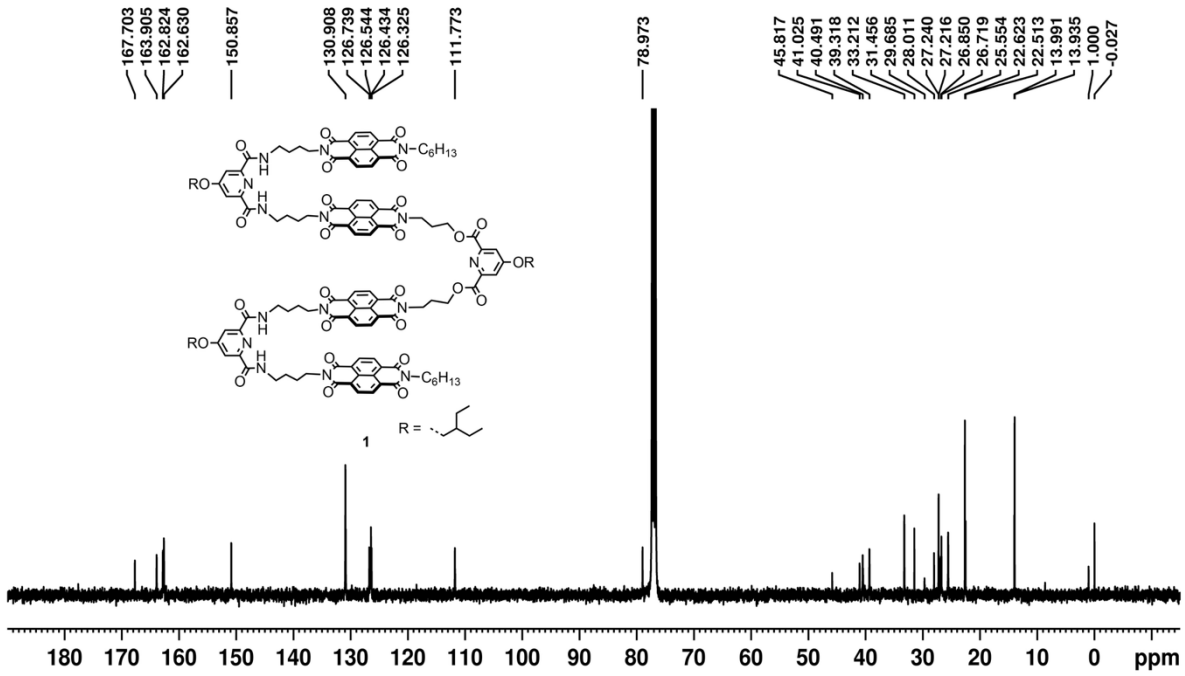

100 MHz, $^{13}C\{1H\}$ NMR of **1** in $CDCl_3$ at 298 K.

6. References

1. J. M. Kumar, I. Huc, Y. Ferrand and B. Gole, *Org. Chem. Front.,* 2025, **12**, 3336-3343.
2. BIOVIA, Dassault Systèmes, FORCITE, San Diego: Dassault Systèmes, [2025].
3. N. Singha , P. Gupta , B. Pramanik, S. Ahmed, A. Dasgupta, A. Ukil and D. Das, *Biomacromolecules*, 2017, **18** , 3630 -3641.
4. T. Wen, J.-Y. Lee, M.-C. Lee, J.-C. Tsai and R.-M. Ho, *Chem. Mater.,* 2017, **29**, 4493-4501